

LEAD ARTICLE

Acta Cryst. (1994). B50, 481–510

Structural Aspects of Oxide and Oxysalt Crystals

BY FRANK C. HAWTHORNE

Department of Geological Sciences, University of Manitoba, Winnipeg, Manitoba, Canada R3T 2N2

(Received 30 July 1993; accepted 23 December 1993)

Frank C. Hawthorne was born in Bristol, England, in 1946, and attended the Royal School of Mines, Imperial College, taking his BSc in Pure Geology. He did his PhD at McMaster University, Hamilton, Ontario, working on the crystal chemistry of the amphiboles using X-ray and neutron diffraction, IR and Mössbauer spectroscopies, and then took a post-doctoral fellowship at the University of Manitoba. He is Professor of Crystallography and Mineralogy in the Department of Geological Sciences at the University of Manitoba, and currently holds a Killam Fellowship. Interests include topological and electronic aspects of crystal structures, solution of unknown mineral structures, all forms of spectroscopy, microbeam analysis, applications of the Rietveld method, crystal chemistry and ordering in complex mineral structures, poetry, art, chocolate and coffee.

Abstract

The goals of theoretical crystallography may be summarized as follows: (1) predict the stoichiometry of the stable compounds; (2) predict the bond topology (*i.e.* the approximate atomic arrangement) of the stable compounds; (3) given the bond topology, calculate accurate bond lengths and angles (*i.e.* accurate atomic coordinates and cell dimensions); (4) given accurate atomic coordinates, calculate accurate static and dynamic properties of a crystal. For oxides and oxysalts, we are now quite successful at (3) and (4), but fail miserably at (1) and (2). The current situation in the first two areas is briefly reviewed, prior to discussing in some detail an approach to topological aspects of structure in oxide and oxysalt crystals. The structure of a molecule or crystal may be represented by a graph, in which the vertices represent orbitals, atoms or groups of atoms, and the edges represent orbital interactions or chemical bonds. The topological characteristics of the bond network are contained in the (weighted) adjacency matrix of the graph and the corresponding eigenvalues constitute the spectrum of the graph. Simple graph theory arguments show that molecular (fundamental) building blocks are actually orbital (or energetic) building blocks, showing that there is an energetic basis for the use of fundamental building blocks in the representation

and hierarchical analysis of complex structures. The electronic energy density of states may be derived by inverting the collection of moments of the energy, which may be evaluated directly from the topology of the bond network. Of particular importance in infinite structures is the observation that the energy difference between two structures is primarily dependent on the first few disparate moments of their respective electron energy density of states. Putting this in structural terms, the important energetic differences between structures involve differences in coordination number and local polyhedral connectivity. This supports the general idea that structures may be hierarchically ordered according to the polymerization of coordination polyhedra with higher bond valences. It is shown that Pauling's rules may be intuitively related to bond topology and its effect on the lower-order moments of the electronic energy density of states. It is also concluded that arguments of ionicity and/or covalency are secondary to the overriding influence of bond topology on the stability and energetics of structure. Bond-valence theory is reviewed in some detail. It may be considered as a simple form of molecular-orbital theory, parameterized via interatomic distance rather than electronegativity or ionization potential, and arbitrarily scaled *via* the valence-sum rule. Combination of bond-valence theory with bond topology/energetic considerations leads to a very simple way of expressing complex structures. The *structural unit* is a strongly bonded, usually anionic, polyhedral array whose charge is balanced by large low-valence *interstitial* cations. This gives a simple binary representation of even the most complicated structure; moreover, we can calculate the Lewis basicity and acidity of the two components and examine their interaction *via* the valence-matching rule. This enables us to examine several aspects of structural chemistry that have hitherto been intractable. The principal idea behind this work is to develop a coherent approach that is reasonably transparent to chemical and physical intuition, and that can be simply applied to complex crystals.

Introduction

Crystallography has been an area of scientific endeavour for at least 350 years. Until the beginning of this century, attention was focused on understanding the morphology, properties and constitution of crystalline materials, together with some inspired speculation as to their internal structure. The discovery of X-ray diffraction in 1912 heralded a major renaissance in crystallography with the demonstration that the arrangements of atoms in (translationally symmetric) solids could be derived. The major thrust initiated at this time has continued to the present day, as nature has provided a spectrum of crystalline materials of increasing complexity that continue to challenge our experimental techniques. However, the success of these experimental techniques has led to the identification of crystallography with the solution and refinement of crystal structures, to the neglect of theoretical approaches aimed at understanding the atomic arrangements observed in crystals and their physical and chemical properties. Although traditionally within the purview of crystallography, such work is now predominantly the domain of solid-state chemists and physicists, much to the detriment of crystallography itself. We still have not progressed very far towards what must be considered as the fundamental goal of crystallography: to predict the structure and properties of a material from a knowledge of its chemical composition. Failure to realize this goal is one of the continuing scandals in the physical sciences (Maddox, 1988), particularly as there is probably more data available for atomic arrangements in crystals than there is in any other area of the physical sciences. The availability of data and the importance of the question make this one of the most pressing scientific problems, and I hope that the following considerations will encourage further effort in this area.

In this article I will focus on oxides and oxysalts in which there are bonds only between unlike atoms; polycompounds are thus excluded. I use the terms 'cation' and 'anion' to denote atoms that are of lesser or greater electronegativity, respectively; these terms carry no implications as to models of chemical bonding.

Theoretical crystallography

We may summarize the goals of *theoretical crystallography* in the following way: Given a chemical system, we wish to

- (1) predict the stoichiometry of the stable compounds;
- (2) predict the bond topology (*i.e.* the approximate atomic arrangement) of these compounds;

- (3) given the bond topology, calculate the accurate bond lengths and angles (*i.e.* accurate atomic coordinates);

- (4) given accurate atomic coordinates, calculate accurate static and dynamic properties of the crystal.

So how successful are we in these matters? The answer to this obviously depends on the complexity of the materials in which we are interested: we can optimize structure and calculate properties far more effectively for a simple oxide or metal than we can for a protein. Here, I am concerned with oxides and oxysalts, perhaps the most tractable group of materials with regard to these problems. However, despite this relative tractability, we are successful only in two of the above four areas. Given an approximate atomic arrangement, we can often calculate atomic positions and physical properties quite well. There are two principal approaches to this problem: (1) potential methods, which recognize the atom as the smallest unit; (2) electronic structure methods, which recognize the electron as the smallest 'unit' and attempt (at some level of approximation) to solve the Schrödinger equation for the system.

The first potential model for crystal structure was developed in the 1920s, primarily by Max Born, with input from Madelung (1918), and involved a simple two-body interatomic potential (Born & Landé, 1918). Deviations from the Cauchy relationship show that a central two-body potential is not sufficient, and current approaches usually include additional noncentral potentials of some form. The Modified Electron Gas (MEG) model (Gordon & Kim, 1972) was introduced for nonempirical determination of repulsive parameters. Detailed developments along these lines are summarized by Burnham (1990) and Catlow & Price (1990). Such models have improved out of all recognition in the last 20 years. They are now capable of predicting structural details, phonon-dispersion relations, elastic properties, thermodynamic data and (most impressively) isotope fractionation factors in such anisodesmic structures as calcite (Dove, Winkler, Leslie, Harris & Salje, 1992) and diopside (Patel, Price & Mendelssohn, 1991).

Electron methods initially involved the use of qualitative molecular-orbital arguments to rationalize observed stereochemistry in molecules in crystals. The success of this approach led to quantitative molecular-orbital calculations on molecular fragments of structures, the fragment being embedded in a field of some sort to simulate the effect of the crystal (Finnis, Paxton, Pettifor, Sutton & Ohta, 1988), and calculations of gradually increasing sophistication (see Tossell & Vaughan, 1992) have significantly increased our understanding of stereochemical variations in crystals. More recently, greatly increased computation power has allowed the

generalization of *ab initio* methods to periodic structures. This can be done either by formulating the molecular orbitals as Bloch functions (Pisani, 1987) or by using Local Density Approximation (LDA) methods (Srivastava & Weaire, 1987). These have been quite successful in calculating elastic constants, equations of state and the electronic structure of reasonably complicated oxides (Dovesi, Pisani, Roetti & Silvi, 1987).

The success of these methods in addressing problems (3) and (4) contrasts with the lack of progress in problems (1) and (2), prediction of the stoichiometry and approximate structure of stable compounds. The rest of this work will consequently focus on the latter areas, in which key-punching is not yet an adequate substitute for arm-waving.

Prediction of stoichiometry of stable compounds

There should be strong connections between the stoichiometry of a stable compound and aspects of its crystal and electronic structure. The one rigorous rule is the principle of electroneutrality: the sum of the formal charges of all the ions in a crystal is zero. However, apart from this one constraint, there have been few additional connections between stoichiometry and structural stability; indeed, there has been little general work in this area.

Dent Glasser (1979) has considered the reasons why many topologically possible silicate structures do not exist. She shows how the topological characteristics of polymerized silicate anions are related to the Lewis basicity of the anion group, and are a function of the field strength of the cation(s) in the structure. In addition, Dent Glasser (1979) proposes that the 'constitutional formulae' of hydrates are such as to minimize the basicity differences between the constituent O atoms, and that Si—O—Si linkages are more stable than protonated groups or silanol groups of low basicity. It is notable that these were the first significant ideas to address the constitution of hydrated structures, and are similar to the ideas of bond-valence theory (Brown, 1981).

The idea of coordination number has been a very fertile one in crystal chemistry. We can think of a crystal structure as a network of chemical bonds with a cation at one end of each bond and an anion at the other. This means that in a chemical compound ${}^{[m]}M_x{}^{[n]}\phi_y$ (where ${}^{[m]}M$ is a cation of coordination number m , and ${}^{[n]}\phi$ is an anion of coordination number n)

$$mx = ny. \quad (1)$$

O'Keeffe & Hyde (1984) use this simple relationship to make some fairly 'strong' observations on coordination numbers, stoichiometry and valence state in simple compounds. Thus, such compounds as

$\text{Na}_{10}\text{Co}_4\text{O}_9$ and K_2NiO_2 (Hoppe, 1981) are stabilized by planar three-coordinate Na and linear two-coordinate Ni, respectively. Similarly, O'Keeffe & Hyde (1984) point out that unusually high oxidation states (*e.g.* Mn^{7+} in KMnO_4 and Ni^{3+} in Na_5NiO_4) are stabilized in ternary metal oxides by decreased cation/anion ratios.

There needs to be much more work done along these lines. It is only by considering a very broad range of materials that any rules governing the occurrence of stable stoichiometries will come to light.

Prediction of approximate atomic arrangements

This is an area in which we fail almost completely. *We cannot a priori predict the structure of even the simplest crystal*; NaCl and MgO remain beyond our grasp. I have stated this in the most uncompromising way in order to emphasize both the fundamental nature of the problem *and* our failure to come to grips with it. Many scientists have not even recognized that the problem is there, and yet it must be the most fundamental problem in crystallography; it deserves more attention.

Having made this 'political statement', it must be said that things are not quite as bad as I have suggested. Within various restricted groups of materials, we can make some predictions based on either an analogy with other materials or *via* topological approaches that operate within (usually very restrictive) boundary conditions.

Structural mapping

We can predict structural arrangements by analogy with other known structures: thus, KCl has the same relative atomic arrangement as NaCl. The idea of different compounds being *isostructural* eventually developed into the method of *structural mapping*, in which crystals with the same stoichiometry could be separated into fields of different structure type by sorting on a small number of (usually) atomic parameters. Different types of atomic radii have been used extensively for this sort of work with varying degrees of success.

Like many important ideas in crystal chemistry, structural mapping was first used by Goldschmidt (1928, 1954). In stoichiometrically simple systems (*e.g.* $A_x\phi_y$, $A_xB_y\phi_z$, where A and B are cations and ϕ are anions), a plot of atomic radii of one species (*e.g.* A) *versus* the radii of another (*e.g.* ϕ) leads to a two-dimensional map in which different structure types tend to form disjoint fields. The simple case of $A\phi$ octet compounds is shown in Fig. 1. As is apparent, the method does a reasonable job of sorting out the four principal structure types of this

group, but fails for seven of the 99 compounds plotted. Also shown on Fig. 1 are the boundaries predicted by the hard-sphere radius-ratio model (Rule 1 of Pauling, 1929); this approach fails to produce an adequate sorting. This result is quite interesting. The use of radii for structural mapping suggests that structural control is dominated by packing considerations. On the other hand, the failure of the hard-sphere model to predict the position of field boundaries on such plots suggests that a 'soft-sphere' model should be more effective, as also implied by more recent attempts to predict coordination numbers in inorganic structures (Brown, 1988). Significant use has been made of such structural maps (Shannon & Prewitt, 1970; Muller & Roy, 1974), but their main utility has been to guide synthesis experiments rather than to explore the reasons for specific structure stabilities. Other atomic parameters have not been as widely used, but Phillips (1970, 1973) sorted the AB -octet compounds into octahedrally coordinated and tetrahedrally coordi-

nated structures on the basis of two parameters representing the covalent (E_h) and ionic (C) parts of the average energy gap (Fig. 2).

Theoretical indices have also been produced and achieve a more successful sorting of simple structure types than the traditional empirical radii. Pseudo-potential radii (Simons & Bloch, 1973; Cohen, 1981; Zunger & Cohen, 1978, 1979; Bloch & Schatterman, 1981) have been quite effective in this regard. The indices R_{σ}^{AB} and R_{π}^{AB} (e.g. Zunger, 1981; Burdett, Price & Price, 1981) are defined as $R_{\sigma}^{AB} = |(r_p^A + r_s^A) - (r_p^B + r_s^B)| = |r_{\sigma}^A - r_{\sigma}^B|$ and $R_{\pi}^{AB} = |r_p^A - r_s^A| + |r_p^B - r_s^B| = |r_{\pi}^A + r_{\pi}^B|$, where r_s^A and r_p^A are the s - and p -orbital radii for atom A . The radii r_{σ}^A and r_{π}^A sort the AB -octet structures (Fig. 3) significantly better than the empirical radii (Fig. 1). As shown by Burdett, Price & Price (1981), these radii are quite good at sorting even quite subtle effects such as inverse *versus* normal spinels.

Despite the success of structural mapping in sorting structure types as a function of properties of their constituent atomic species, it is necessary to emphasize that it does not predict the structure of a

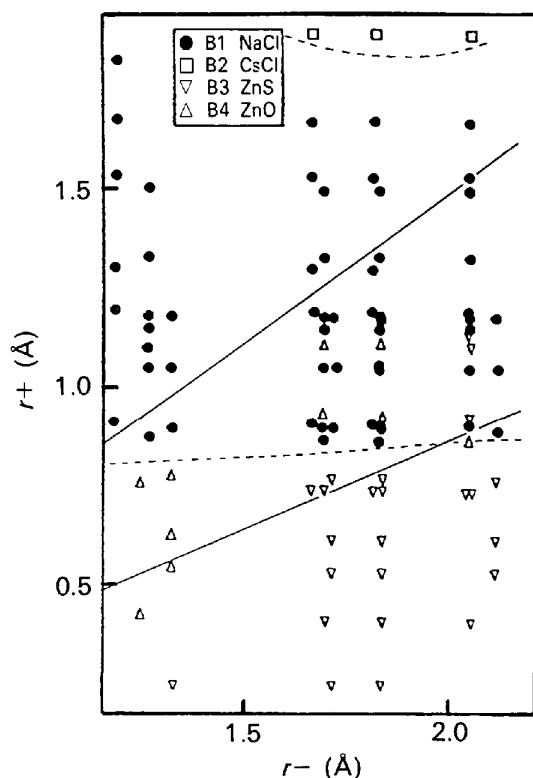


Fig. 1. Structural map for 99 AB -octet compounds using the radii (corresponding to the observed coordination number) from Shannon (1976); ● = NaCl structure-type; □ = CsCl structure-type; ▽ = ZnS structure-type; △ = ZnO structure-type. The solid lines show the field boundaries according to the (hard-sphere) radius-ratio rules; the broken lines best sort the data into four-, six- and eight-coordination fields; after Burdett, Price & Price (1981).

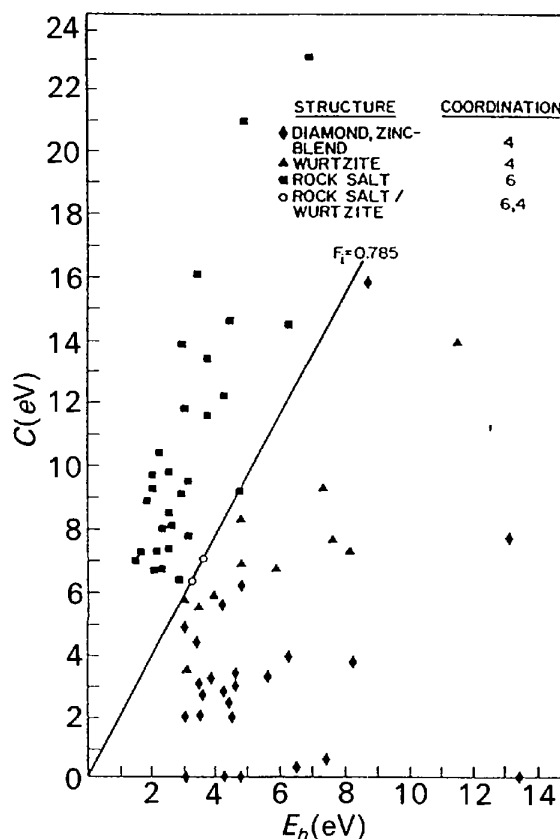


Fig. 2. Structural map for four-coordination and six-coordination AB compounds using the covalent (E_h) and ionic (C) parts of the average energy gap; legend as in Fig. 1, after Phillips (1970).

compound *except* by analogy with other known structures. Nevertheless, this approach should have much to contribute to our understanding of what features actually determine the relative stabilities of simple structure types.

Nets and tetrahedral framework structures

Two-dimensional (O'Keeffe & Hyde, 1980) and three-dimensional nets (Wells, 1956, 1970, 1977, 1984) have long been used to describe crystal structures. However, they have only seen extensive predictive use in the area of tetrahedral framework structures, particularly zeolites (Smith, 1988). Smith (1977) considered possible ways to link planar three-connected 6^3 nets in the third dimension to form four-connected three-dimensional nets as predictive models for tetrahedral framework structures (Fig. 4). The ensuing 15 years have seen extensive use of this approach for structure prediction (see review by Smith, 1988). This has been of particular importance with regard to zeolite structures. Synthetic zeolites and zeolitic materials are of considerable industrial importance as molecular sieves and catalysts, and knowledge of their structures is of great importance

in optimization of their use. However, these synthetic materials are often only very fine-grained and normal single-crystal crystallographic techniques cannot be used (except where synchrotron facilities are available). Consequently, structure solution and refinement must proceed *via a priori* structure prediction (within the constraint of known cell dimensions) and Rietveld structure refinement.

Wood & Price (1992) have shown how to systematically generate two-dimensional three-connected plane nets. Combination with the stacking operators of Akporiaye & Price (1989) could result in a fairly automated generation of four-connected three-dimensional nets. This, of course, begs the next question of how do we select the physically realizable structures from the extremely large number of nets generated by this procedure. In this regard, Brunner & Meier (1989) have shown that zeolite and zeolite-type structures have a lower limit on the framework density (number of tetrahedral nodes [atoms] per 1000 \AA^3), a limit that is strongly dependent on the size of the smallest (tetrahedral) rings in the structure.

These techniques have been quite successful in deriving structural details for quite complicated zeolite and zeolite-like structures. Of more general interest is the question: what specific aspects of a net make it the basis of a stable atomic arrangement relative to other nets that are not the basis of observed structures? The ability to systematically generate all possible four-connected three-

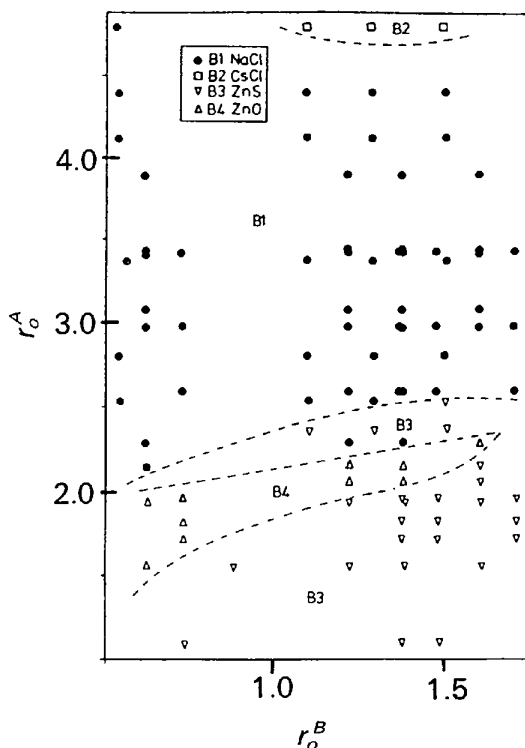


Fig. 3. Structural map for the $A\phi$ -octet compounds using combinations of pseudopotential atomic radii, r_o^A and r_o^B (see text), of Bloch & Schattman (1981); legend as in Fig. 1, after Burdett, Price & Price (1981).

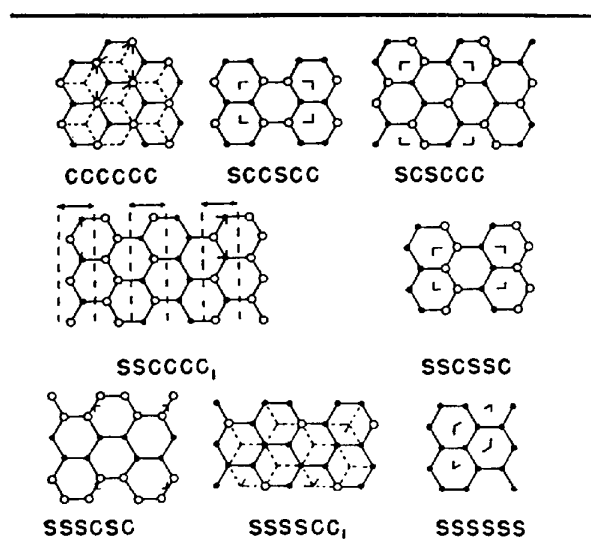


Fig. 4. Simple ways of adding a vertical linkage to each node of a 6^3 net to give a four-connected three-dimensional net. The letters S and C denote whether a linkage is the same or different from adjacent linkages; after Smith (1977).

dimensional nets (subject to unit-cell volume restrictions to make the problem finite) indicates that a systematic approach to this question is now possible.

Crystal structures as graphs

The usual representations of a crystal structure are:

(1) unit-cell and symmetry information, plus a table of atom coordinates;

(2) a structure drawing that is usually based on assumptions as to which atoms are bonded together.

Using (1), we can perform various structure-property calculations, provided that we have sufficient computing power and appropriate potentials or wave functions; the problem is that this representation offers little intuitive feel for the factors controlling structural stability. Using representation (2), we can make qualitative arguments (*e.g.* à la Pauling's rules), but we do not have a quantitative expression of the important features of a structure. Graph theory offers a potential solution to some of these problems.

Fig. 5 shows four atoms; the lines represent chemical bonds between these atoms. This representation, a set of points joined by lines, is the visual representation of a graph. Formally, we may define a *graph* as a nonempty set of elements, $V(G)$, called vertices, and a nonempty set of unordered pairs of these vertices, $E(G)$, called edges. If we let the vertices of the graph represent atoms (as in Fig. 5) or groups of atoms, and the edges of the graph represent chemical bonds (or linkages between groups of atoms), then our graph may represent a molecule. We can introduce an algebraic representation of this graph in the form of a matrix (Fig. 5). Each column and row of the matrix is associated with a specific (labeled) vertex and the corresponding matrix entries denote whether or not two vertices are adjacent, that is joined by an edge. If the edges of the graph are weighted in some form such that the matrix elements denote this weighting, then this matrix is called the

adjacency matrix. The adjacency matrix is thus a digital representation of the graph, which is in turn an analogue representation of the structure. The adjacency matrix does not preserve the geometrical features of the structure; information such as bond angles is lost. However, it does preserve information concerning the *topological* features of the bond network, with the possibility of carrying additional information concerning the strengths (or orders) of the chemical bonds.

We have introduced a way of quantifying the topological aspects of the bond network of a group of atoms. It remains to determine the significance of this information. To do this, we now examine some of the connections that have recently developed between contemporary theories of chemical bonding and topological (or graphical) aspects of structure. I shall only sketch the outlines of the arguments, except where they serve to emphasize the equivalence or similarity between energetics of bonding and topological aspects of structure. Excellent reviews are given by Burdett (1980), Albright, Burdett & Whangbo (1985) and Hoffmann (1988).

Topological aspects of molecular-orbital theory

Molecules

A reasonable first approach to the electronic structure and properties of molecules is to consider a molecule as the sum of the electronic properties of its constituent atoms, as modified by the interaction between these atoms. The most straightforward way of doing this is to construct the molecular-orbital wavefunction from a *Linear Combination of Atomic Orbitals* (LCAO method) of the chemist and the tight-binding method of the physicist. These wavefunctions are eigenstates of some (unspecified) effective one-electron Hamiltonian, H^{eff} , that we may write as

$$H^{\text{eff}}\psi = E\psi, \quad (2)$$

where E is the energy (eigenvalue) associated with ψ , and the LCAO molecular-orbital wavefunction is written as

$$\psi = \sum_i c_i \varphi_i \quad (3)$$

where $\{\varphi_i\}$ are the valence orbitals of the atoms of the molecule and c_i is the contribution of a particular atomic orbital to a particular molecular orbital.

The total electron energy of the state described by this wavefunction may be written as

$$\begin{aligned} E &= (\int \psi^* H^{\text{eff}} \psi d\tau) / (\int \psi^* \psi d\tau) \\ &= (\langle \psi | H^{\text{eff}} | \psi \rangle) / (\langle \psi | \psi \rangle), \end{aligned} \quad (4)$$

in which the integration is over all space. Substitution of (3) into (4) gives

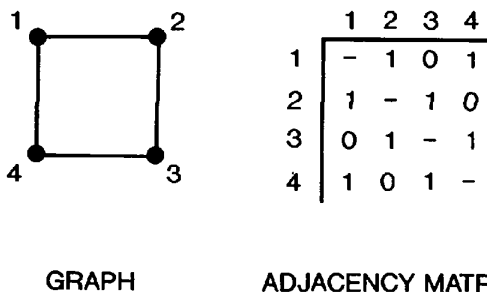


Fig. 5. A hypothetical molecule consisting of four atoms (●) joined by chemical bonds (—); as drawn, this is a labeled graph (left). An algebraic representation of this graph is the adjacency matrix (right).

$$E = (\sum_i \sum_j c_i c_j \langle \varphi_i | H^{\text{eff}} | \varphi_j \rangle) / (\sum_i \sum_j c_i c_j \langle \varphi_i | \varphi_j \rangle). \quad (5)$$

This equation may be simplified by the following substitutions and approximations:

(a) $\langle \varphi_i | \varphi_j \rangle$ is the overlap integral between atomic orbitals on different atoms; we will denote this as S_{ij} , and note that it is always ≤ 1 ; when $i = j$, $\langle \varphi_i | \varphi_j \rangle = 1$ for a normalized (atomic) basis set of orbitals.

(b) We write $\langle \varphi_i | H^{\text{eff}} | \varphi_i \rangle = H_{ii}$; this is the Coulomb integral and represents the energy of an electron in orbital φ_i . It can be approximated by the orbital ionization potential.

(c) We write $\langle \varphi_i | H^{\text{eff}} | \varphi_j \rangle = H_{ij}$; it represents the interaction between orbitals φ_i and φ_j and is the *resonance integral*. It can be approximated by the Wolfsberg-Helmholz relationship $H_{ij} = KS_{ij}(H_{ii} + H_{jj})/2$ (Gibbs, Hamil, Louisnathan, Bartell & Yow, 1972).

We may obtain the molecular-orbital energies from (5) *via* the variational theorem, minimizing the energy with respect to the coefficients c_i . The most familiar form is the following *secular determinant* equation, the eigenvalues (roots) of which give the molecular-orbital energy levels

$$|H_{ij} - S_{ij}E| = 0. \quad (6)$$

Here we will consider the Hückel approximation (Trinajstić, 1983), as this most directly shows the topological content of this approach. In the Hückel approximation, all H_{ii} values for the $p\pi$ orbitals are set equal to α , all H_{ij} are set equal to β , and all S_{ij} ($i \neq j$) are set equal to zero. As an example, consider cyclobutadiene (Fig. 6). Writing out the secular determinant equation in full, we obtain

$$\begin{vmatrix} \alpha - E & \beta & 0 & \beta \\ \beta & \alpha - E & \beta & 0 \\ 0 & \beta & \alpha - E & \beta \\ \beta & 0 & \beta & \alpha - E \end{vmatrix} = 0. \quad (7)$$

The matrix entries in (7) may be compared with the cyclobutadiene structure of Fig. 6. The diagonal terms ($\alpha - E$) can be thought of as the 'self-interaction' terms; in the absence of any off-diagonal β terms, there are no chemical bonds formed, and the roots of the equation are the energies of the electrons in the atomic orbitals themselves. When chemical bonding occurs, these energies are modified by the off-diagonal β terms. Thus, when two atoms are bonded together (*i.e.* atoms 1 and 2 in Fig. 6), there is a nonzero value at this particular (1,2) entry in the secular determinant; when two atoms are not bonded together (*i.e.* atoms 1 and 3 in Fig. 6), then the corresponding determinant entry (1,3) is zero. Referring to Fig. 5, we see that this description is very similar to the adjacency matrix of the corre-

sponding graph. If we use the normalized form of Hückel theory, in which β is taken as the energy unit, and α is taken as the zero-energy reference point (Trinajstić, 1983), then the determinant of (7) becomes identical to the corresponding adjacency matrix. The eigenvectors of the adjacency matrix are identical to the Hückel molecular orbitals. Hence, *it is the topological (graphical) characteristics of a molecule, rather than any geometrical details, that determine the form of the Hückel molecular orbitals*. For cyclobutadiene, the orbital energies found from the secular determinant [*i.e.* the four roots of (7)] are $E = \alpha + 2\beta$, α ($\times 2$) and $\alpha - 2\beta$. These are shown in Fig. 6, both in a conventional energy representation, and as a *density-of-states* diagram.

Molecular building blocks

When dealing with very complicated problems, we often resolve them into simple (usually additive or weakly interacting) components that are easier to handle. Molecular and crystal structures are no exception; we recognize structural building blocks and build hierarchies of structures using these 'molecular bricks'. Let us consider this from a graph theoretical point of view.

A graph G' is a subgraph of a graph G if the vertex and edge sets $V(G')$ and $E(G')$ are subsets of the vertex and edge sets $V(G)$ and $E(G)$; this is illustrated in Fig. 7. We may express any graph as the sum of a set of subgraphs. The eigenvalues of each subgraph G' are a subset of the eigenvalues of the main graph G , and the eigenvalues of the main graph are the sum of the eigenvalues of all the subgraphs. In the last section, we saw that the eigenvalues of an adjacency matrix are identical to the Hückel molecular orbitals. Now let us consider the construction of large molecules from smaller building blocks. This provides us with a convenient visual way of analyzing the connectivity of our molecule, and of relating molecules together. But this is not all. The fact that the eigen-

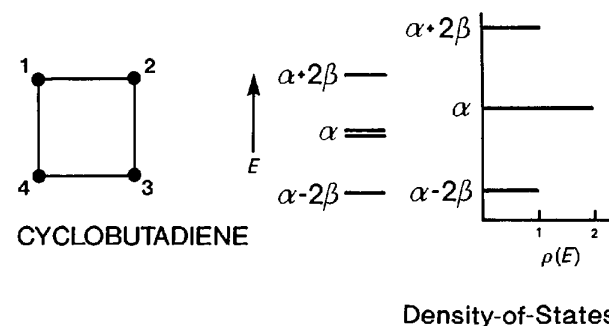


Fig. 6. The cyclobutadiene molecule (left); to the right are the four roots of equation (6), the electron energy levels are expressed in the usual form (centre) and in a density-of-states form (right).

values of the graphs of our building blocks are contained in the eigenvalues of the graph of the complete molecule indicates that we may consider our building blocks as *orbital* or *energetic* building blocks. Thus, there is an energetic basis for the use of fundamental building blocks (FBBs) in the representation and hierarchical analysis of complex structures.

Crystals

We can conceive of constructing a crystal from constituent molecular building blocks, in this way considering the crystal as a giant molecule. However, it is not clear what influence translational periodicity will have on the energetics of this conceptual building process. To try to clarify this problem, we will now examine the energetic differences between a molecule and a crystal.

What would happen if we were able to solve (7) for a giant molecule? The results are sketched in Fig. 8. Solution of the secular determinant will give a very large number of molecular-orbital energies, and obviously their conventional representation solely as a function of energy is not very useful; such results are better expressed as a density-of-states diagram (Fig. 8), in which the electron occupation of a specific energy interval (band) is expressed as a function of orbital energy.

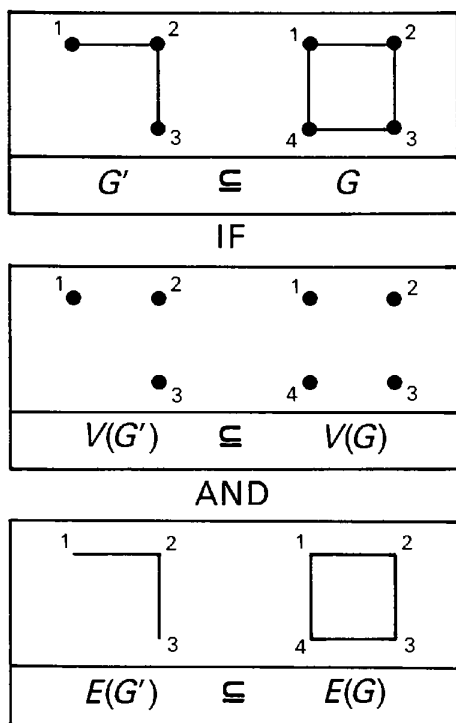


Fig. 7. The relationship between a graph G and a subgraph G' expressed in terms of the relevant vertex- and edge-sets

So what happens in a crystal which has translational symmetry? Obviously we cannot deal with a crystal using the same sort of calculation, as there are approximately Avogadro's number of atoms in a (macroscopic) crystal, far beyond any foreseeable computational capability. Instead, we must make use of the translational symmetry to reduce the problem to a manageable size. We do this by using *Bloch orbitals* (Ziman, 1965), in which the orbital content of the unit cell is constrained to the periodicity of the crystal. The secular determinant is solved at a representative set of points within the Brillouin zone (the *special-points method*), giving a (hopefully) representative sampling of the orbital energy levels that may be smoothed to give the usual density-of-states representation. The total orbital energy can then be calculated by integrating the electronic energy density-of-states up to the Fermi level.

The differences between a molecule and a crystal may thus be summarized as follows: in a molecule, there is a discrete set of orbital energy levels; in a crystal, these levels broaden into bands whose occupancies as a function of energy are represented by the corresponding electronic energy density-of-states.

The method of moments

The usual method for deriving the electronic energy density-of-states has little intuitive connection to what we usually think of as the essential features of a crystal structure, the relative positions of the atoms and the disposition of the chemical bonds. In this regard, Burdett, Lee & Sha (1984) have come up with a very important method of deriving the electronic energy density-of-states using the *method of moments*. I will give only a brief outline of the method; interested readers should consult the original paper for mathematical details, and are also referred to Burdett (1986, 1987) for further applications in solid-state chemistry.

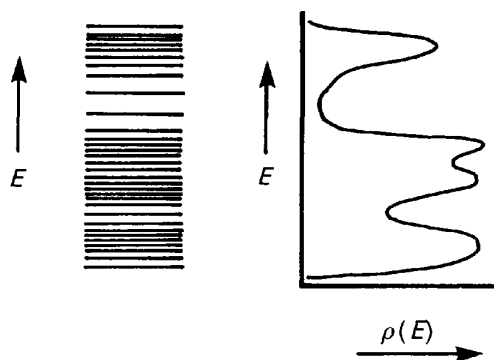


Fig. 8. The electron energy levels for a giant molecule expressed in the usual way (left) and in a density-of-states form (right).

To solve the secular determinant (7), we diagonalize the Hamiltonian matrix. The trace of this matrix may be expressed as

$$\text{Tr}(H^n) = \sum_i \sum_{j,k,\dots,n} H_{ij}H_{jk}\cdots H_{ni}. \quad (8)$$

A topological (graphical) interpretation of one term in this sum is shown in Fig. 9. Each H_{ij} term is the interaction integral between orbitals i and j , and hence is equal to β (if the atoms are bonded) or zero (if the atoms are not bonded, or if $i = j$ when $\alpha = 0$). Thus, a single term $\{H_{ij}H_{ik}\cdots H_{in}\}$ in (8) is nonzero only if all H_{ij} terms are nonzero. As the last H_{ij} term is the interaction between the n th orbital and the first orbital, the $\{H_{ij}H_{jk}\cdots H_{ni}\}$ term represents a closed path of length n in the graph of the orbitals (molecule). In Fig. 9, the term $\{H_{ij}H_{jk}H_{kl}H_{li}\}$ represents the clockwise path of length 4 around the cyclobutadiene $p\pi$ orbitals. Thus, the complete sum of (8) represents all circuits of length n through the graph of (the orbital structure of) the molecule.

The trace of the Hückel matrix remains invariant under diagonalization, and thus

$$\text{Tr}(H^n) = \text{Tr}(E^n) = \mu_n, \quad (9)$$

where E is the diagonal matrix of eigenvalues (energy levels) and μ_n is the n th moment of E , formally denoted by

$$\mu_n = \sum_i E_i^n. \quad (10)$$

The collection of moments $\{\mu_n\}$ may be inverted [see Burdett, Lee & Sha (1984) for mathematical details] to give the density-of-states. As we can evaluate $\text{Tr}(H^n)$ directly from the topology of the orbital interactions (bond topology), we thus derive the electronic energy density-of-states *directly* from the bond topology. Of course, we have already shown that this is the case by demonstrating the equivalence of the secular determinant and the adjacency matrix of the molecule. However, the method of moments

generalizes quite readily to infinite systems (*i.e.* crystals).

For an infinite system, we can define the n th moment of E as

$$\mu_n = \int E^n \rho(E) dE, \quad (11)$$

where $\rho(E)$ is the density-of-states. In principle, the moments may be evaluated as before and inverted to give the electronic energy density-of-states. Thus, we see, in principle, the topological content of the electronic energy density-of-states in an infinite system, which in turn emphasizes the energetic content of a topological (graphical) representation of periodic structure. However, we can go further than this. Burdett (1986) has shown that the energy difference between two structures can be expressed in terms of the first few disparate moments of their respective electronic energy density-of-states. Thus, when comparing two structures, *the important energetic terms are the most local topological differences between the structures*. Putting this in structural terms, the important energetic terms involve differences in coordination number (including ligand type) and differences in local polyhedral linkage. Furthermore, in structures with bonds of different strengths, each edge of each path (walk) that contributes to each moment will be weighted according to the value of the strength (resonance integral) of the bond defining that edge. Thus, strongly bonded paths through the structure will contribute more to the moments of the electronic energy density-of-states than weakly bonded paths. The most important energetic features of a structure are thus not only the local connectivity, but the local connectivity of the strongly bonded coordination polyhedra in the structure. This provides energetic justification for a hypothesis that will be introduced later on, that structures may be ordered according to the polymerization of the more strongly bonded coordination polyhedra (Hawthorne, 1983).

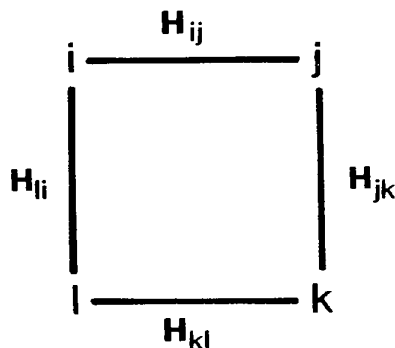


Fig. 9. Topological interpretation of a single term in the sum of equation (7); for each orbital i , the nonzero terms are a series of circuits of length n with orbital i as the origin; the term shown here has $n = 4$ (for cyclobutadiene).

Topological aspects of crystal chemistry

The stability of inorganic crystals is governed (sometimes weakly) by a set of rules that dates back to early work on the electronic theory of valence (Lewis, 1916, 1923) and the structure of crystals. The most rigorous rule is that of electroneutrality: *the sum of the formal charges of all the ions in a crystal is zero*. Although we tend to take this rule for granted, it is an extremely powerful constraint on possible chemical variations in crystals. Other rules grew out of observations on a few mineral and inorganic structures. Barlow [as described by Bragg, (1955, pp. 270–271)] predicted the structure of NaCl on the basis of sphere-packing arguments long before the discovery of X-ray diffraction. Bragg's (1913) solu-

tion of the structure of halite vindicated Barlow's arguments and the idea of structures as close packings of spheres became useful in the solution of crystal structures. Bragg (1921) introduced the idea that atoms have a certain size, and produced a table of atomic radii. Bragg (1930) also introduced the idea of coordination number and considered silicate minerals as polymerizations of coordination polyhedra. These ideas were refined by Pauling (1929, 1960), who systematized them into his well known rules for the behavior of 'complex ionic crystals':

(1) A coordination polyhedron of anions is formed about each cation, the cation-anion distance being determined by the radius sum and the ligancy (coordination number) of the cation being determined by the radius ratio.

(2) The strength of a bond from a cation to an anion is equal to the cation charge divided by the cation coordination number; in a stable (ionic) structure, the formal valence of each anion is approximately equal to the sum of the incident bond strengths.

(3) The presence of shared faces and edges between coordination polyhedra decreases the stability of a structure; this effect is large for cations of large valence and small ligancy.

(4) In a crystal containing different cations, those with large valence and small coordination number tend not to share polyhedral elements with each other.

These rules put some less rigorous constraints on the behavior of structures, constraints that are traditionally associated with the ionic model of the chemical bond; they allow us to make the following type of statements about the structure and chemistry of inorganic crystals:

(a) the formula is electrically neutral;

(b) we may make (weak) predictions of likely coordination numbers from the radius ratio rules;

(c) we can make fairly good ($< 0.02 \text{ \AA}$) predictions of mean bond lengths by summing ionic radii.

Compared with the enormous amount of structural and chemical data available, our predictive capabilities concerning this information is limited in the extreme. The following questions are pertinent in this regard:

(a) Within the constraint of electroneutrality, why do some stoichiometries occur whereas others do not?

(b) Given a specific stoichiometry, what is its bond connectivity (bond topology)?

(c) Given a specific stoichiometry and bond connectivity, what controls the site occupancies?

These are some of the basic questions that need answering if we are going to understand and be able to predict the stability of inorganic atomic arrangements.

Pauling's rules

Let us consider how each of Pauling's rules relates to the topology of the bond connectivity in crystals.

Rule (1). The mean interatomic distance in a coordination polyhedron can be determined by the radius sum. This point has been extensively developed up to the present (Shannon, 1976; Baur, 1987; O'Keeffe & Brese, 1991), together with consideration of additional factors that also affect mean bond lengths in crystals (Shannon, 1975; Baur, 1981). The first rule also states that the coordination number is determined by the radius ratio. This works reasonably well for small high-valence cations, but does not work well for large low-valence cations. For example, inspection of Shannon's (1976) table of ionic radii shows Na radii listed for coordination numbers from 4 to 12 with oxygen ligands, whereas a radius-ratio criterion would indicate that any cation can have (at most) only two coordination numbers for a specific anion. It is important to note that the coordination number of an atom is one of the lowest moments of the electronic energy density-of-states.

Rule (2). This is also known (rather unfortunately) as the electrostatic valence rule. It has been further extended by Baur (1970, 1971), who developed a scheme for predicting individual bond lengths in crystals, given the bond connectivity, and by Brown & Shannon (1973), who quantitatively related the length of a bond to its strength (bond valence). The latter scheme has proved a powerful *a posteriori* method of examining crystal structures for crystal chemical purposes. This rule relates strongly to the local connectivity of strong bonds in a structure and again involves significant low-order moments of the electronic energy density-of-states.

Rules (3) and (4). Both of these rules again relate to the local connectivity in a structure, and strongly affect the important low-order moments, both by different short paths resulting from different local bond topologies, and from differences in *anion* coordination numbers.

These arguments show that Pauling's rules can all be intuitively related to bond topology and its effect on the low-order moments of the electronic energy density-of-states.

Ionicity and covalency

Pauling's rules were presented as *ad hoc* generalizations, rationalized by qualitative arguments based on an electrostatic model of the chemical bond. This led to an association of these rules with the ionic model, and there has been considerable criticism of the second rule as an 'unrealistic' model for bonding in most solids. Nevertheless, these rules have been too useful to discard and, in various modifications, continue to be used to the present day. Clearly, their

proof is in their applicability to real structures rather than in the details of somewhat vague ionic arguments (Burdett & McLarnan, 1984).

There has been significant progress in the past 15 years in both rationalizing and predicting geometrical aspects of structures from a molecular-orbital viewpoint (Burdett, 1980; Gibbs, 1982; Tossell & Gibbs, 1977). In particular, it has been shown that many of the geometrical predictions of Pauling's rules can also be rationalized by molecular-orbital calculations on small structural fragments. Burdett & McLarnan (1984) show how the same predictions from Pauling's rules can be rationalized in terms of band-structure calculations, again focusing on the covalent interactions, but doing so for an infinite structure. It is interesting to note how these two approaches parallel the arguments given previously concerning the relationship between bond topology and energetics:

(1) the energy of a molecular fragment is a function of its topological characteristics *via* the form of the secular determinant;

(2) the electronic energy density-of-states of a continuous structure can be expressed in terms of the sum of the moments of the energy density-of-states, which is related to the topological properties of its bond network.

The thread that links these ideas together is the topology of the bond network *via* its effect on the energy of the system. This also parallels our earlier conclusion that all of Pauling's rules relate to the topological characteristics of the bond network of a crystal.

Consider two (dimorphic) structures of the same stoichiometry but different atomic arrangement. As the chemical formulae of the two structures are the same, the *atomic* components of the energy of each structure must be the same, and the difference in energy between the two structures must relate *completely* to the difference in bond connectivity. This 'general principles' argument emphasizes the importance of bond topology in structural stability and finds more specific expression in the method of moments developed by Burdett, Lee & Sha (1984). Thus, we come to the general conclusion that *arguments of ionicity and/or covalency in structure are secondary to the overriding influence of bond topology on the stability and energetics of structure.*

Bond-valence theory

Brown (1981, 1992) and O'Keeffe (1989, 1990) have developed a simple yet coherent approach to chemical bonding in inorganic structures, based on Pauling's second rule and its more quantitative generalization by Brown & Shannon (1973).

Although empirical bond-valence curves are now widely used, the general ideas of bond-valence theory have not yet seen the use that they deserve. I shall briefly review these ideas, as they can be developed further to deal in a very simple way with many aspects of complex inorganic structures that cannot be approached by other methods.

Bond-valence relationships

According to Pauling's second rule (Pauling, 1960), bond strength, p , is defined as

$$p = \text{cation valence/cation coordination number} = Z/cn. \quad (12)$$

Summing the bond strengths around the anions, the second rule states that the sum should be approximately equal to the magnitude of the anion valence

$$\sum_{\text{anion}} p \sim |Z_{\text{anion}}|. \quad (13)$$

Correlations between deviations from Pauling's second rule and bond-length variations in crystals have been parameterized for specific cation-anion bonds (see Allmann, 1975). For such schemes, I use the term *bond valence*, in contrast to the Pauling scheme for which I use the term *bond strength*; this is merely a convenient nomenclature without any other significance.

Brown & Shannon (1973) expressed bond valence, s , as a function of bond length, R , in the following way

$$s = s_o |R/R_o|^{-N} \text{ or } s = |R/R_1|^{-n}, \quad (14)$$

where s_o , R_o , N , R_1 and n are constants characteristic of cation-anion pairs, and were derived by fitting such equations to a large number of well-refined crystal structures under the constraint that the valence-sum rules work as closely as possible. In (14), R_o is nominally a refined parameter, but is obviously equal to the grand mean bond length for the particular bond pair and cation coordination number under consideration; s_o is equal to the Pauling bond strength. Thus, $(R/R_o) \sim 1$ and s_o is actually a scaling factor that ensures that the sum of the bond valences around an atom is approximately equal to the magnitude of its valence.

Suppose that there is a delocalization of charge into the bonds, together with a reduction in the charge on each atom. For an $A-B$ bond, let the residual charges change by $Z_A p_A$ and $Z_B p_B$, respectively. The (Pauling) bond strength [= scaling constant s_o in (14)] is given by $Z_A p_A / cn$, where cn is the coordination number of atom A . Inserting these values into (14) and summing over the bonds around B gives

$$\sum_B = p_A \sum s_o |R/R_o|^{-N} = p_B |Z_B|. \quad (15)$$

If $p_A \sim p_B$, these terms cancel and the bond-valence equation works, provided the relative delocalization of charge from each formally ionized atom is not radically different. Thus, the bond-valence equation can apply from 'very ionic' to 'very covalent' situations.

Bond-valence theory as a molecular-orbital model

There has been considerable criticism of Pauling's second rule and its more recent extensions; criticisms based on its perception as a description of ionic bonding. In this regard, Bragg (1930) produced an interesting argument to justify Pauling's second rule. He considered the (nearest-neighbor) forces that bond atoms together into coordination polyhedra, conceptually modeling the interactions by 'lines of force'. He noted that atoms that are closer together will have more lines of force between them, atoms that are further apart will have less lines of force, and that next-nearest neighbors can interact only through their nearest-neighbors. The 'charge' of the bond strength was associated with the bond between two atoms and the amount of charge was inversely related to the bond length. This sounds much more like a molecular-orbital description of bonding than an ionic description, allowing for the unconventional vocabulary used in the argument.

In their original work, Brown & Shannon (1973) emphasized the difference between bond-valence theory and the ionic model. In bond-valence theory, the structure consists of a series of atomic cores held together by valence electrons that are associated with the chemical bonds between atoms; they also explicitly state that the valence electrons may be associated with chemical bonds in a symmetric (covalent) or asymmetric (ionic) manner. However, *a priori* knowledge of the electron distribution is not necessary, as it is quantitatively derived from the application of the bond-valence curves to the observed structure. Indeed, Burdett & Hawthorne (1993) show how the bond-valence bond-length relationship may be derived algebraically from a molecular-orbital description of a solid in which there is a significant energy gap between the interacting orbitals on adjacent atoms. *Thus, we may consider bond-valence theory as a very simple form of molecular-orbital theory, parameterized via interatomic distance rather than electronegativity or ionization potential, and (arbitrarily) scaled via the valence-sum rule.*

Network solids

Let us define a crystal, liquid or molecule as a network of atoms connected by chemical bonds. For the materials in which we are interested, any path through this network contains alternating cations and anions, and the total network is subject to the

law of electroneutrality: the total valence of the cations is equal to the total valence of the anions. A bond valence can be assigned to each bond such that the *valence-sum rule* is obeyed: *the sum of the bond valences at each atom is equal to the magnitude of the atomic valence*. If the interatomic distances are known, then the bond valences can be calculated from the curves of Brown (1981); if the interatomic distances are not known, then the bond valences can be approximated by Pauling's bond strengths.

Characteristic bond valences

So far, we have been dealing with formalizations from and extensions of Pauling's rules. Although these ideas are important, they are an *a posteriori* analysis: the structure must be known in detail before we can apply these ideas. This is obviously not satisfactory. We need an *a priori* approach to structure stability if we are to develop any predictive capability. In this regard, Brown (1981) introduced a very important idea. If we examine the bond valences around a specific cation in a wide range of crystal structures, we find that the values lie within *ca* 20% of the mean value; this mean value is thus characteristic of that particular cation. If the cation only occurs in one type of coordination, then the mean bond valence for that cation will be equal to the Pauling bond strength; thus, P always occurs in tetrahedral coordination to O, and will hence have a mean bond valence of $5/4 = 1.25$ v.u. If the cation has more than one coordination number, then the mean bond valence will be equal to the weighted mean of the bond valences in all the observed structures. Thus, Fe^{2+} occurs in various coordinations from 4 to 8; the tendency is for four- and five-coordinations to be more common than seven- and eight-coordinations, and hence the mean bond valence is 0.40 v.u.

As the mean bond valence correlates with formal charge and cation size, it should vary systematically through the periodic table; this is in fact the case. Table 1 shows these values, smoothed across the periods and down the groups of the periodic table.

Lewis acid and base strengths

The mean bond valence of a cation correlates strongly with its *electronegativity* (Fig. 10). Conceptually, this is not surprising. The electronegativity is a measure of the electrophilic strength (electron-accepting capacity) of the cation and the correlation with its characteristic bond valence (Fig. 10) indicates that the latter is a measure of the *Lewis acid strength* of the cation (see also O'Keeffe & Brese, 1991). Thus, we have the following definition (Brown, 1981):

Table 1. Lewis acid strengths (v.u.) for cations

Li	0.22	Sc	0.50	Cu ²⁺	0.45
Be	0.50	Ti ³⁺	0.50	Zn	0.36
B	0.88	Ti ⁴⁺	0.75	Ga	0.50
C	1.30	V ³⁺	0.50	Ge	0.75
N	1.75	V ⁵⁺	1.20	As	1.02
Na	0.16	Cr ³⁺	0.50	Se	1.30
Mg	0.36	Cr ⁶⁺	1.50	Rb	0.10
Al	0.63	Mn ²⁺	0.36	Sr	0.24
Si	0.95	Mn ³⁺	0.50	Sn	0.66
P	1.30	Mn ⁴⁺	0.67	Sb	0.86
S	1.65	Fe ²⁺	0.36	Te	1.06
Cl	2.00	Fe ³⁺	0.50	Cs	0.08
K	0.13	Co ²⁺	0.40	Ba	0.20
Ca	0.29	Ni ²⁺	0.50	Pb ²⁺	0.20

Values taken from Brown (1981), except Pb²⁺ which was estimated from several oxysalt mineral structures.

The Lewis acid strength of a cation may be defined as the characteristic (bond) valence = atomic (formal) valence/mean coordination number.

We can define the Lewis base strength of an anion in exactly the same way, as the characteristic valence of the bonds formed by the anion. However, bond-valence variations around anions are much greater than those around cations. For example, the valences of the bonds to O²⁻ vary between nearly zero and 2.0 v.u.; thus, in Na[Al(SO₄)₂(H₂O)₆].(H₂O)₆ (Cromer, Kay & Larsen, 1967), Na is in 12-coordination and the O atom to which it is bonded receives 0.08 v.u. from the Na—O bond; conversely in CrO₃ (Stephens & Cruickshank, 1970), one O is bonded only to Cr⁶⁺ and receives 2.00 v.u. from the Cr—O bond. With this kind of variation, it is not particularly useful to define a Lewis base strength for a simple anion such as O²⁻.

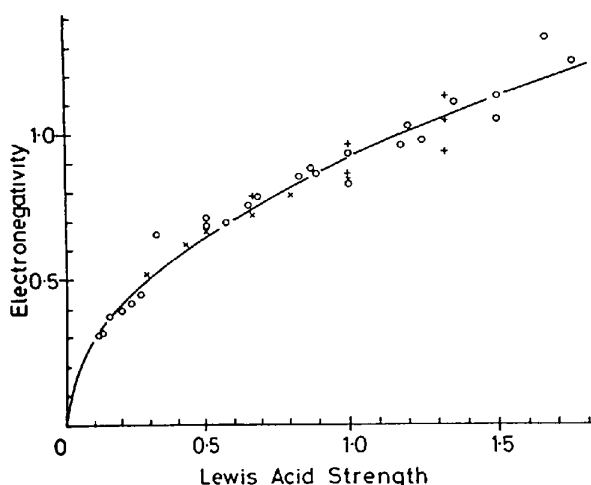


Fig. 10. Lewis acid strength (mean bond valence for a specific cation) as a function of cation electronegativity (from Brown, 1981); circles are main-group elements in their highest oxidation state, crosses (×, +) are the same elements in lower oxidation states.

Table 2. Lewis basicities (v.u.) for selected oxyanions

(BO ₃) ³⁻	0.33	(CO ₃) ²⁻	0.25
(SiO ₄) ⁴⁻	0.33	(NO ₃) ³⁻	0.12
(AlO ₄) ³⁻	0.42	(VO ₄) ³⁻	0.25
(PO ₄) ³⁻	0.25	(SO ₄) ²⁻	0.17
(AsO ₄) ³⁻	0.25	(CrO ₄) ²⁻	0.17

The situation is entirely different if we consider complex oxyanions. Consider the (SO₄)²⁻ oxyanion shown in Fig. 11. Each O atom receives 1.5 v.u. from the central S⁶⁺ cation and hence each O atom of the group needs an additional 0.5 v.u. to be supplied by additional cations. If the O coordination number is [n], then the average valence of the bonds to O²⁻ (exclusive of the S—O bond) is 0.5/(n - 1) v.u.; thus, if n = 2, 3, 4 or 5, then the mean bond valences to the O are 0.50, 0.25, 0.17 or 0.11 v.u., respectively. As all the O atoms in the (SO₄)²⁻ oxyanion have the same environment, then the average bond valence received by the oxyanion is the same as the average bond valence received by the individual O atoms. In this way, we can define the Lewis basicity of an oxyanion. Note that for the (SO₄)²⁻ oxyanion discussed above, the possible average bond valences are quite tightly constrained (0.50–0.11 v.u.) and we can easily calculate a useful Lewis basicity. Table 2 lists Lewis basicities for some common inorganic oxyanions.

The valence-matching principle

The definitions of Lewis acid and base strengths lead to a specific criterion for chemical bonding, the valence-matching principle:

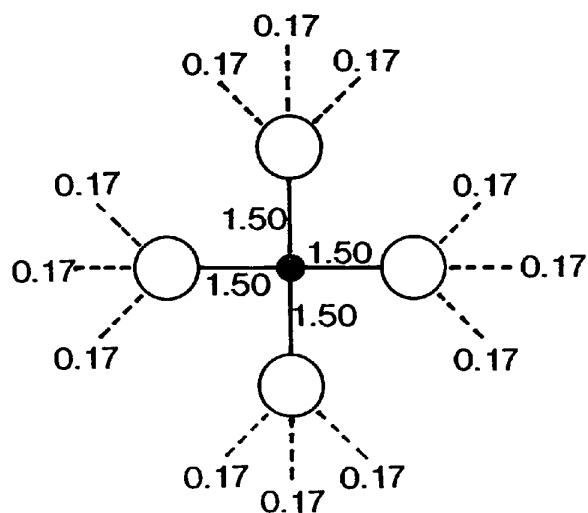


Fig. 11. Bond-valence structure of the (SO₄)²⁻ oxyanion, with the individual bond valences shown in v.u.; ● = sulphur, ○ = oxygen.

The most stable structures will form when the Lewis acid strength of the cation closely matches the Lewis base strength of the anion.

We can consider this as the chemical analogue of the handshaking principle in combinatorial mathematics and the 'kissing' principle in social relationships. As a chemical bond contains two constituents, then the properties of the constituents must match for a stable configuration to form.

Simple applications of the valence-matching principle

Na_2SO_4 (Hawthorne & Ferguson, 1975a) illustrates both the utility of defining a Lewis base strength for an oxyanion and the working of the valence-matching principle (Fig. 11). As outlined above, the bond valences to O^{2-} vary between 0.17 and 1.50 v.u. Assuming a mean O coordination number of 4, the Lewis basicity of the $(\text{SO}_4)^{2-}$ oxyanion is 0.17 v.u., which agrees very well with the Lewis acidity of 0.16 v.u. for Na given in Table 1. Thus, the Na— (SO_4) bond is in accordance with the valence-matching principle and Na_2SO_4 is a stable structure.

Consider the formula Na_4SiO_4 . The Lewis basicity of the $(\text{SiO}_4)^{4-}$ oxyanion is 0.33 v.u. (Table 2) and the Lewis acidity of Na is 0.17 v.u. These values do not agree and thus a stable bond cannot form; consequently, Na_4SiO_4 is not a very stable material.

Consider the formula Ca_2SiO_4 . The Lewis basicity of $(\text{SiO}_4)^{2-}$ is 0.33 v.u. and the Lewis acidity of Ca is 0.29 v.u. These values agree reasonably well and Ca_2SiO_4 is stable as the mineral larnite.

Consider the formula CaSO_4 . The relevant Lewis basicity and acidity are 0.17 and 0.29 v.u., respectively; according to the valence-matching principle, we do not expect a stable structure to form. However, the mineral anhydrite is stable, the cation and anion coordination numbers both reducing to allow the structure to satisfy the valence-sum rule (Hawthorne & Ferguson, 1975b). However, anhydrite hydrates readily in the presence of water to produce gypsum, $\text{CaSO}_4 \cdot (\text{H}_2\text{O})_2$; this instability is suggested by the violation of the valence-matching principle.

These simple examples illustrate the power of the valence-matching principle as a simple way in which we can consider the possibility of cation-anion interactions of interest. It is important to recognize that this is an *a priori* analysis, rather than the *a posteriori* analysis of Pauling's second rule and its various modifications.

A hierarchical approach to structure

The utility of organizing crystal structures into hierarchical sequences has long been recognized. Bragg

(1930) classified the silicate minerals according to the way in which the (SiO_4) tetrahedra polymerize, and this scheme was generalized to polymerized tetrahedral structures by Zoltai (1960) and Liebau (1985). Further developments along similar lines were the classifications of the aluminium hexafluoride minerals (Pabst, 1950; Hawthorne, 1984a) and the borate minerals (Christ, 1960; Christ & Clark, 1977). Such an approach to hierarchical organization is of little use in such chemical groups as the phosphates or the sulphates, in which the principal oxyanion does not self-polymerize. Moore (1984) developed a classification of phosphate minerals, based on the polymerization of divalent and trivalent metal octahedra. However, all these hierarchical schemes focus on specific chemical classes of compounds and are not easily adapted to other classes.

We can approach this general problem within the framework of bond-valence theory. First let us consider the cations in a structure. The cation bond-valence requirements are satisfied by the formation of anion coordination polyhedra around them. Thus, we can think of a structure as an array of complex anions that polymerize in order to satisfy their (simple) anion bond-valence requirements according to the valence-sum rule. Let the bond valences in an array of coordination polyhedra be represented by s_o^i ($i = 1, n$), where $s_o^i > s_o^{i+1}$. The valence-sum rule indicates that polymerization can occur when

$$s_o^1 + s_o^n < |V_{\text{anion}}| \quad (16)$$

and the valence-sum rule is most easily satisfied when

$$s_o^1 + s_o^n = |V_{\text{anion}}|. \quad (17)$$

This suggests that the most important polymerizations involve those coordination polyhedra with higher bond valences, subject to the constraint of (17), as these linkages most easily satisfy the valence-sum rule (under the constraint of maximum volume).

A general hypothesis

Hawthorne (1983) has proposed the following hypothesis:

Structures may be hierarchically ordered according to the polymerization of coordination polyhedra with higher bond valences.

There are two important points to be made with regard to this idea:

(1) we define the structural elements by bond valences rather than by chemistry; consequently, there is no division of structures into different chemical groups, except as occurs naturally *via* the different 'strengths' of the chemical bonds.

(2) Earlier, we argued that the topology of the bond network is a major feature controlling the energy of a structure. The polymerization of the

principal coordination polyhedra is merely another way of expressing the topology of the bond network. Thus, at the intuitive level, we can recognize an energetic basis for the hierarchical organization of structures according to the details of their polyhedral polymerization.

Dimensional polymerization

Families of complex structures are often based on different arrangements of a *fundamental building block* (FBB). This is a tightly-bonded unit within the structure and can be envisaged as the inorganic analogue of a molecule in an organic structure. The FBB is usually a *homo-* or *heteropolyhedral cluster* of coordination polyhedra with the strongest bond-valence linkages in the structure. The FBB is repeated, usually polymerized, to form the *structural unit*, a complex anionic polyhedral array whose charge is balanced by the presence of large low-valence *interstitial* cations (usually alkalis or alkaline earths). These definitions are illustrated for the mineral tornebohmite in Fig. 12. The following nomenclature is used here: $M \geq$ five-coordinate, $T =$ three- or four-coordinated, $\phi =$ unspecified anion.

The various structural units can be arranged according to the mode of polymerization:

(a) Unconnected polyhedra, (b) finite clusters, (c) infinite chains, (d) infinite sheets and (e) infinite frameworks.

As will be shown later, hydrogen-containing groups [e.g. $(\text{OH})^-$, $(\text{H}_2\text{O})^\ominus$] often exert a major control on the dimensional character of the structural unit (Hawthorne, 1992). Most work has focused on structures with triangles, tetrahedra and octahedra as principal coordination components of the structural unit (Hawthorne, 1979, 1984a, 1985a, 1986, 1990; Eby & Hawthorne, 1993; Moore, 1970a,b, 1973, 1974, 1975, 1982, 1984; Lima de Faria, 1983; Lima de Faria & Figueiredo, 1976),

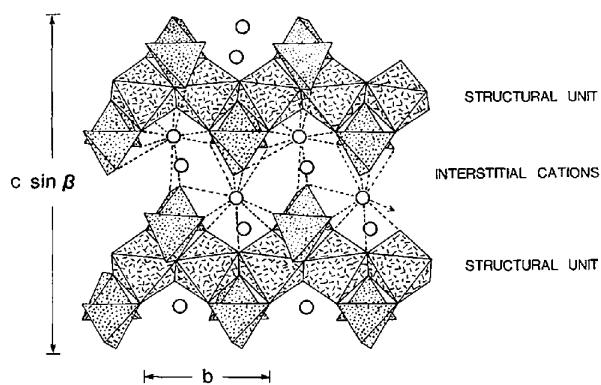


Fig. 12. The structural unit and the interstitial species in tornebohmite.

although there has been some notable work (Moore, 1981) on structures with important higher coordination numbers. The following outline cannot, of course, be comprehensive, but it is hopefully representative of the diversity shown by these types of structures. I shall focus on the structures of minerals for several reasons. First, much work of this type has involved mineral structures. Second, this restriction provides a reasonable sampling of inorganic oxysalt structures, from simple close-packed oxides to very complicated quasi-zeolitic hydroxy-hydrated oxysalts. There are certain regularities that become apparent when structures are examined in this fashion. I shall draw attention to these without necessarily providing an explanation; indeed, many of these features are, as yet, unexplained, but they all indicate nature's economy of effort when it comes to structural design in crystals.

Unconnected-polyhedra structures

In crystals of this class, low-coordination oxyanions [e.g. $(\text{SO}_4)^{2-}$, $(\text{PO}_4)^{3-}$, $(\text{CO}_3)^{2-}$, $(\text{NO}_3)^-$ and $(\text{TeO}_4)^{2-}$] and intermediate coordination complex cations [e.g. $\{\text{Mg}(\text{H}_2\text{O})_6\}$ and $\{\text{Al}(\text{H}_2\text{O})_5\text{F}\}$] are linked together by large low-valence interstitial cations and by hydrogen bonding; thus, the (H_2O) group usually plays a major role in the structural chemistry of this particular class of structures. Tetrahedral cations are coordinated by oxygens and octahedral cations are coordinated predominantly by (H_2O) groups; the exceptions to the latter are khademite and the minerals of the fleischerite group (Table 3), in which the octahedral groups are $[\text{Al}(\text{H}_2\text{O})_5\text{F}]$ and $[\text{Ge}(\text{OH})_6]$, respectively. It is notable that khademite is the only $M(T\phi_4)\phi_n$ structure (in this class) with a trivalent octahedral cation; all other compounds have divalent octahedral cations. Similarly, the fleischerite-group minerals are the only $M(T\phi_4)_2\phi_n$ minerals (in this class) with tetravalent octahedral cations; all other minerals of this stoichiometry have trivalent octahedral cations.

From an inspection of Table 3, some rules governing the compositions of these isolated polyhedra structures become apparent. The Lewis basicity of the $(T\phi_4)$ group must be low (*i.e.* < 0.20 v.u.), otherwise the valence-matching principle forces it to bond to a strong Lewis acid and form a polymerized structural unit. Thus, these compounds are predominantly sulphates (or other hexavalent TO_4 salts). When a pentavalent T cation (such as P or As) occurs, it does so as an acid (PO_3OH) group; it is notable that such acid pentavalent-cation groups have a Lewis basicity of 0.18 v.u. [very similar to the value of 0.17 v.u. for the hexavalent (TO_4) groups and significantly different from the Lewis basicity of 0.25 v.u. for the (PO_4) group]. The only exception is

Table 3. Selected $M(T\phi_4)\phi_n$, $M(T\phi_4)_2\phi_n$ and $M_x(T\phi_3)_y\phi_z$ minerals based on unconnected polyhedra

$M(T\phi_4)\phi_n$ mineral	Formula	Space group	$M(T\phi_4)_2\phi_n$ mineral	Formula	Space group
Bianchite	$[\text{Zn}(\text{H}_2\text{O})_6][\text{SO}_4]$	$C2/c$	Amarillite	$\text{Na}[\text{Fe}^{3+}(\text{SO}_4)_2(\text{H}_2\text{O})_6]$	$P2_1/a$
Ferrohexahydrate	$[\text{Fe}^{2+}(\text{H}_2\text{O})_6][\text{SO}_4]$	$C2/c$	Tamarugite	$\text{Na}[\text{Al}(\text{SO}_4)_2(\text{H}_2\text{O})_6]$	$P2_1/a$
Hexahydrate	$[\text{Mg}(\text{H}_2\text{O})_6][\text{SO}_4]$	$C2/c$	Mendozite	$\text{Na}[\text{Al}(\text{SO}_4)_2(\text{H}_2\text{O})_6](\text{H}_2\text{O})_6$	$C2/c$
Moorhouseite	$[\text{Co}(\text{H}_2\text{O})_6][\text{SO}_4]$	$C2/c$	Kalinite	$\text{K}[\text{Al}(\text{SO}_4)_2(\text{H}_2\text{O})_6](\text{H}_2\text{O})_6$	$C2/c$
Nickel hexahydrate	$[\text{Ni}(\text{H}_2\text{O})_6][\text{SO}_4]$	$C2/c$	Sodium alum	$\text{Na}[\text{Al}(\text{SO}_4)_2(\text{H}_2\text{O})_6](\text{H}_2\text{O})_6$	$Pa3$
Retgersite	$[\text{Ni}(\text{H}_2\text{O})_6][\text{SO}_4]$	$P4_2,2,2$	Potassium alum	$\text{K}[\text{Al}(\text{SO}_4)_2(\text{H}_2\text{O})_6](\text{H}_2\text{O})_6$	$Pa3$
Khademite	$[\text{Al}(\text{H}_2\text{O})_6\text{F}][\text{SO}_4]$	$Pcab$	Tschermigite	$\text{NH}_4[\text{Al}(\text{SO}_4)_2(\text{H}_2\text{O})_6](\text{H}_2\text{O})_6$	$Pa3$
Epsomite	$[\text{Mg}(\text{H}_2\text{O})_6][\text{SO}_4](\text{H}_2\text{O})$	$P2_1,2,2$	Apjohnite	$\text{Mn}[\text{Al}(\text{SO}_4)_2(\text{H}_2\text{O})_6](\text{H}_2\text{O})_{10}$	$P2_1/c$
Goslarite	$[\text{Zn}(\text{H}_2\text{O})_6][\text{SO}_4](\text{H}_2\text{O})$	$P2_1,2,2$	Bilinite	$\text{Fe}^{2+}[\text{Fe}^{3+}(\text{SO}_4)_2(\text{H}_2\text{O})_6](\text{H}_2\text{O})_{10}$	$P2_1/c$
Morenosite	$[\text{Ni}(\text{H}_2\text{O})_6][\text{SO}_4](\text{H}_2\text{O})$	$P2_1,2,2$	Dietrichite	$\text{Zn}[\text{Al}(\text{SO}_4)_2(\text{H}_2\text{O})_6](\text{H}_2\text{O})_{10}$	$P2_1/c$
Bierberite	$[\text{Co}(\text{H}_2\text{O})_6][\text{SO}_4](\text{H}_2\text{O})$	$P2_1/c$	Halotrichite	$\text{Fe}^{2+}[\text{Al}(\text{SO}_4)_2(\text{H}_2\text{O})_6](\text{H}_2\text{O})_{10}$	$P2_1/c$
Boothite	$[\text{Cu}(\text{H}_2\text{O})_6][\text{SO}_4](\text{H}_2\text{O})$	$P2_1/c$	Pickeringite	$\text{Mg}[\text{Al}(\text{SO}_4)_2(\text{H}_2\text{O})_6](\text{H}_2\text{O})_{10}$	$P2_1/c$
Mallardite	$[\text{Mn}(\text{H}_2\text{O})_6][\text{SO}_4](\text{H}_2\text{O})$	$P2_1/c$	Redingtonite	$\text{Fe}^{2+}[\text{Cr}(\text{SO}_4)_2(\text{H}_2\text{O})_6](\text{H}_2\text{O})_{10}$	$P2_1/c$
Melanterite	$[\text{Fe}^{2+}(\text{H}_2\text{O})_6][\text{SO}_4](\text{H}_2\text{O})$	$P2_1/c$	Aubertite	$\text{Cu}^{2+}[\text{Al}(\text{SO}_4)_2(\text{H}_2\text{O})_6]\text{Cl}(\text{H}_2\text{O})_6$	$P\bar{1}$
Zinc melanterite	$[\text{Zn}(\text{H}_2\text{O})_6][\text{SO}_4](\text{H}_2\text{O})$	$P2_1/c$	Boussingaultite	$(\text{NH}_4)_2[\text{Mg}(\text{SO}_4)_2(\text{H}_2\text{O})_6]$	$P2_1/c$
Phosphorroesslerite	$[\text{Mg}(\text{H}_2\text{O})_6][\text{PO}_3(\text{OH})](\text{H}_2\text{O})$	$C2/c$	Cyanochroite	$\text{K}_2[\text{Cu}^{2+}(\text{SO}_4)_2(\text{H}_2\text{O})_6]$	$P2_1/c$
Roesslerite	$[\text{Mg}(\text{H}_2\text{O})_6][\text{AsO}_3(\text{OH})](\text{H}_2\text{O})$	$C2/c$	Mohrite	$(\text{NH}_4)_2[\text{Fe}^{2+}(\text{SO}_4)_2(\text{H}_2\text{O})_6]$	$P2_1/c$
Struvite	$\text{NH}_4[\text{Mg}(\text{H}_2\text{O})_6][\text{PO}_4]$	$Pmn2_1$	Picromerite	$\text{K}_2[\text{Mg}(\text{SO}_4)_2(\text{H}_2\text{O})_6]$	$P2_1/c$
			Despujolsite	$\text{Ca}_3[\text{Mn}^{2+}(\text{SO}_4)_2(\text{OH})_6](\text{H}_2\text{O})_6$	$P\bar{6}2c$
			Fleischerite	$\text{Pb}_3[\text{Ge}(\text{SO}_4)_2(\text{OH})_6](\text{H}_2\text{O})_6$	$P\bar{6}2c$
			Schauertite	$\text{Ca}_3[\text{Ge}(\text{SO}_4)_2(\text{OH})_6](\text{H}_2\text{O})_6$	$P\bar{6}2c$

struvite which has a (PO_4) group (Table 3). However, struvite has $(\text{NH}_4)^+$ as the interstitial complex-cation species and $(\text{NH}_4)^+$ has a Lewis acidity of 0.25 v.u. (Table 1); thus, solely because of the nature of the interstitial cation in struvite, this mineral can have an isolated (PO_4) group. Hence, bond-valence considerations seem to account quite nicely for the compositional characteristics of these isolated-polyhedral structures.

Finite-cluster structures

Selected compounds of this class are given in Table 4, and the different types of clusters found in these minerals are illustrated in Fig. 13.

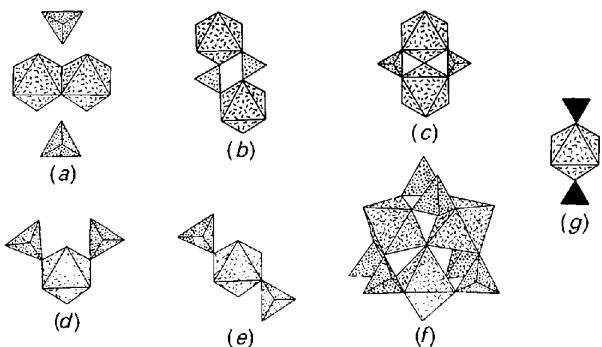


Fig. 13. Finite polyhedral clusters in $[M(T\phi_4)\phi_4]$ and $[M(T\phi_4)_2\phi_n]$ structures: (a) the $[M_2(T\phi_4)_2\phi_{10}]$ cluster in jurbanite; (b) the $[M_2(T\phi_4)_2\phi_8]$ cluster in the rozenite group minerals; (c) the $[M_2(T\phi_4)_2\phi_7]$ cluster in morinitite; (d) the *cis*- $[M(T\phi_4)_2\phi_4]$ cluster in roemerite; (e) the *trans*- $[M(T\phi_4)_2\phi_4]$ cluster in anapaite, bloedite, leonite and schertelite; (f) the $[M_3(T\phi_4)_6\phi_4]$ cluster in metavoltine; (g) the $[M(T\phi_3)_2\phi_4]$ cluster in baylissite.

Table 4. $M(T\phi_4)\phi_n$, $M(T\phi_4)_2\phi_n$ and $M_x(T\phi_3)_y\phi_z$ minerals based on finite clusters of $M\phi_6$ octahedra, $T\phi_4$ tetrahedra and $T\phi_3$ triangles

$M(T\phi_4)\phi_n$	Formula	Space group	Fig.
Jurbanite	$[\text{Al}(\text{SO}_4)(\text{OH})(\text{H}_2\text{O})_4](\text{H}_2\text{O})$	$P2_1/n$	13a
Aplowitzite	$[\text{Co}(\text{SO}_4)(\text{H}_2\text{O})_4]$	$P2_1/n$	13b
Boyleite	$[\text{Zn}(\text{SO}_4)(\text{H}_2\text{O})_4]$	$P2_1/n$	13b
Ilesite	$[\text{Mn}(\text{SO}_4)(\text{H}_2\text{O})_4]$	$P2_1/n$	13b
Rozenite	$[\text{Fe}^{2+}(\text{SO}_4)(\text{H}_2\text{O})_4]$	$P2_1/n$	13b
Starkeyite	$[\text{Mg}(\text{SO}_4)(\text{H}_2\text{O})_4]$	$P2_1/n$	13b
Morinitite	$\text{Ca}_2\text{Na}[\text{Al}_2(\text{PO}_4)_2\text{F}_4(\text{OH})(\text{H}_2\text{O})_2]$	$P2_1/m$	13c
$M_x(T\phi_3)_y\phi_z$ mineral	Formula		
Baylissite	$\text{K}_2[\text{Mg}(\text{CO}_3)_2(\text{H}_2\text{O})_4]$	$P2_1/n$	13g
Anapaite	$\text{Ca}_2[\text{Fe}^{2+}(\text{PO}_4)_2(\text{H}_2\text{O})_4]$	$P\bar{1}$	13e
Bloedite	$\text{Na}_2[\text{Mg}(\text{SO}_4)_2(\text{H}_2\text{O})_4]$	$P2_1/a$	13e
Leonite	$\text{K}_2[\text{Mg}(\text{SO}_4)_2(\text{H}_2\text{O})_4]$	$C2/m$	13e
Schertelite	$(\text{NH}_4)_2[\text{Mg}(\text{PO}_3\text{OH})_2(\text{H}_2\text{O})_4]$	$Pbca$	13e
Roemerite	$\text{Fe}^{2+}[\text{Fe}^{3+}(\text{SO}_4)_2(\text{H}_2\text{O})_4](\text{H}_2\text{O})_6$	$P\bar{1}$	13d
Metavoltine	$\text{K}_2\text{Na}_6\text{Fe}^{2+}[\text{Fe}^{3+}(\text{SO}_4)_6(\text{H}_2\text{O})_4]_2(\text{H}_2\text{O})_2$	$P3$	13f

In jurbanite (Sabelli, 1985a), the cluster consists of an octahedral edge-sharing dimer of the form $[\text{Al}_2(\text{OH})_2(\text{H}_2\text{O})_8]$ and an isolated (SO_4) tetrahedron [Fig. 13(a)]. These two fragments are bound together by hydrogen bonding from the octahedral dimer (donor) to the tetrahedron (acceptor) and hence, jurbanite is actually transitional between the unconnected polyhedra structures and the finite-cluster structures.

In the $M(T\phi_4)\phi_n$ minerals, the structures of the members of the rozenite group are based on the $[M_2(T\phi_4)_2\phi_8]$ cluster [Fig. 13(b)], linked solely by hydrogen bonding between adjacent clusters. The morinitite structure (Hawthorne, 1979) is based on the $[M_2(T\phi_4)_2\phi_7]$ cluster [Fig. 13(c)], linked by interstitial

cations as well as interunit hydrogen bonds. Hawthorne (1983) derived all possible finite clusters of the form $[M_2(T\phi_4)_2\phi_n]$ with no linkage between tetrahedra and with only corner-sharing between tetrahedra and octahedra. Based on the conjecture that the more stable clusters are those in which the maximum number of anions have their bond-valences most nearly satisfied, four clusters were predicted to be the most stable; two of these are the clusters of Figs. 13(b) and (c).

There is far more structural variety in the $M(T\phi_4)_2\phi_n$ minerals (Table 4). Anapaite, bloedite, leonite and schertelite are based on the simple $[M(T\phi_4)_2\phi_4]$ cluster of Fig. 13(d), linked by a variety of interstitial cations and hydrogen-bond arrangements (Hawthorne, 1985c). Roemerite (Fanfani, Nunzi & Zanazzi, 1970) is also based on an $[M(T\phi_4)_2\phi_4]$ cluster, but in the *cis* rather than in the *trans* arrangement [Fig. 13(e)]. Metavoltine (Giacovazzo, Scordari, Todisco & Menchetti, 1976) is built from a complex but elegant $[M_3(T\phi_4)_6\phi_4]$ cluster [Fig. 13(f)] that is also found in a series of synthetic compounds investigated by Scordari (1980, 1981). Again it is notable that the $M(T\phi_4)_2\phi_n$ minerals in this class are characterized by interstitial cations, whereas the bulk of the $M(T\phi_4)\phi_n$ minerals are not, as was the case for the unconnected polyhedra structures.

Baylissite (Bucat, Patrick, White & Willis, 1977) is based on an $[M(T\phi_3)_2\phi_4]$ finite cluster [Fig. 13(g)] that resembles the $[M(T\phi_4)_2\phi_4]$ cluster [Fig. 13(e)]. These clusters pack together to form rather open sheets that are similar to the cluster packings in the analogous $[M(T\phi_4)_2\phi_4]$ cluster compounds (Hawthorne, 1985c).

The energetic considerations outlined previously suggest that the stability of these finite-cluster struc-

tures will be dominated by the topological aspects of their connectivity. Nevertheless, it is apparent from the structures of Table 4 that this is not the only significant aspect of their stability. Fig. 14 shows the structures of most of the minerals of Table 4. It is very striking that these clusters pack in essentially the same fashion, irrespective of their nature, and irrespective of their interstitial species. Although a more detailed examination of this point is desirable, its very observation indicates that not only does nature choose a very small number of fundamental building blocks, but she also is very economical in her ways of linking them together.

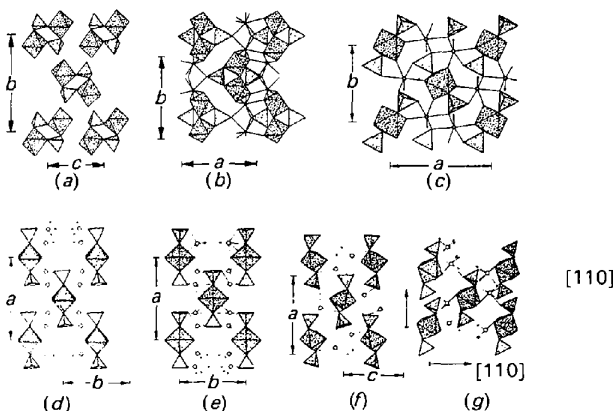


Fig. 14. Selected finite cluster structures of $[M(T\phi_4)\phi_n]$ and $[M(T\phi_4)_2\phi_n]$ stoichiometry: (a) rozenite; (b) morinite; (c) bloedite; (d), (e) leonite; (f) schertelite; (g) anapaite.

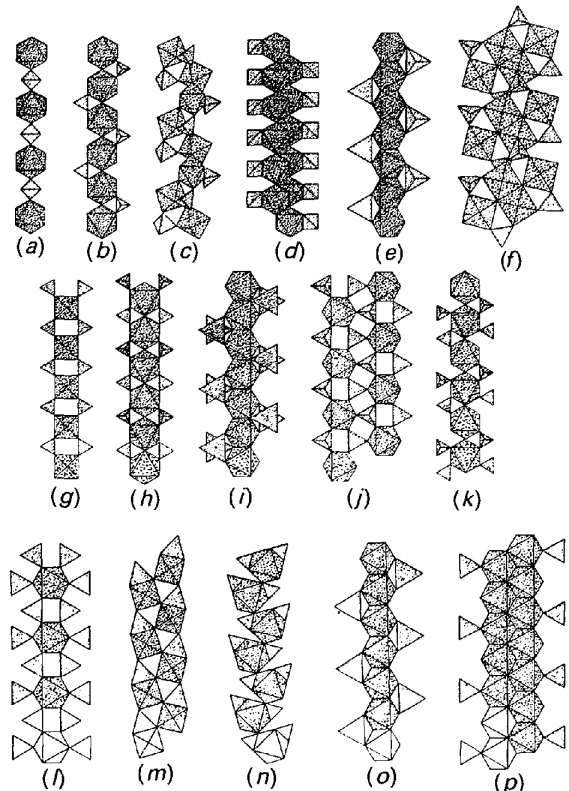


Fig. 15. Infinite chains in $[M(T\phi_4)\phi_n]$ and $[M(T\phi_4)_2\phi_n]$ structures: (a) the $[M(T\phi_4)\phi_4]$ chain in the chalcantite-group minerals, lironite and brassite; (b) the $[M(T\phi_4)\phi_3]$ chain in butlerite, parabutlerite, the childrenite group and uklonskovite; (c) the $[M(T\phi_4)\phi_3]$ chain in fibroferrite; (d) the $[M(T\phi_4)\phi]$ chain in chlorotianite; (e) the $[M(T\phi_4)\phi_2]$ chain in the linarite-group minerals; (f) the $[M_2(T\phi_4)_4\phi_2]$ chain in amaranite and hohmannite; (g) the $[M(T\phi_4)_2\phi_2]$ chain in the krohnkite, talnessite and fairfieldite groups; (h) the $[M(T\phi_4)_2\phi]$ chain in tancoite, sideronatrite, the jahnite and segelerite groups, guildite and yftsite; (i) the $[M(T\phi_4)_2\phi]$ chain in the brackebuschite, fornacite and vauquelinite groups; (j) the $[M(T\phi_4)_2\phi]$ chain in ransomite and krausite; (k) the $[M_2(T\phi_4)_4\phi_2]$ chain in botryogen; (l) the $[M(T\phi_3)_4]$ chain in sahamalite; (m) the $[M(T\phi_3)_2\phi_2]$ chain in nesquehonite; (n) the $[M(T\phi_3)\phi]$ chain in chalconatronite; (o) the $[M(T\phi_3)_2\phi_2]$ chain in dundasite; (p) the $[M_2(T\phi_3)_4\phi_2]$ chain in artinite.

Table 5. $M(T\phi_4)\phi_n$, $M(T\phi_4)_2\phi_n$ and $M_x(T\phi_3)_y\phi_z$ minerals based on infinite chains of $M\phi_6$ octahedra, $T\phi_4$ tetrahedra and $T\phi_3$ triangles

$M(T\phi_4)\phi_n$ mineral	Formula	Space group	Fig.	$M(T\phi_4)_2\phi_n$ mineral	Formula	Space group	Fig.
Chalcanthite	$[\text{Cu}(\text{SO}_4)(\text{H}_2\text{O})_4](\text{H}_2\text{O})$	$P\bar{1}$	15a	Brandtite	$\text{Ca}_2[\text{Mn}(\text{AsO}_4)_2(\text{H}_2\text{O})_2]$	$P2_1/c$	15g
Jokokuite	$[\text{Mn}(\text{SO}_4)(\text{H}_2\text{O})_4](\text{H}_2\text{O})$	$P\bar{1}$	15a	Krohnkite	$\text{Na}_2[\text{Cu}(\text{SO}_4)_2(\text{H}_2\text{O})_2]$	$P2_1/c$	15g
Pentahydrate	$[\text{Mg}(\text{SO}_4)(\text{H}_2\text{O})_4](\text{H}_2\text{O})$	$P\bar{1}$	15a	Roselite	$\text{Ca}_2[\text{Co}(\text{AsO}_4)_2(\text{H}_2\text{O})_2]$	$P2_1/c$	15g
Siderotil	$[\text{Fe}^{2+}(\text{SO}_4)(\text{H}_2\text{O})_4](\text{H}_2\text{O})$	$P\bar{1}$	15a	Cassidyite	$\text{Ca}_2[\text{Ni}(\text{PO}_4)_2(\text{H}_2\text{O})_2]$	$P\bar{1}$	15g
Liroconite	$\text{Cu}_2[\text{Al}(\text{AsO}_4)(\text{OH})_4](\text{H}_2\text{O})_4$	$I2/a$	15a	Collinsite	$\text{Ca}_2[\text{Mg}(\text{PO}_4)_2(\text{H}_2\text{O})_2]$	$P\bar{1}$	15g
Brassite	$[\text{Mg}(\text{AsO}_3(\text{OH}))(\text{H}_2\text{O})_4]$	$Pbca$	15a	Gaitite	$\text{Ca}_2[\text{Zn}(\text{AsO}_4)_2(\text{H}_2\text{O})_2]$	$P\bar{1}$	15g
Butlerite	$[\text{Fe}^{3+}(\text{SO}_4)(\text{OH})(\text{H}_2\text{O})_2]$	$P2_1/m$	15b	Roselite-beta	$\text{Ca}_2[\text{Co}(\text{AsO}_4)_2(\text{H}_2\text{O})_2]$	$P\bar{1}$	15g
Parabutlerite	$[\text{Fe}^{3+}(\text{SO}_4)(\text{OH})(\text{H}_2\text{O})_2]$	$Pmnb$	15b	Talmessite	$\text{Ca}_2[\text{Mg}(\text{AsO}_4)_2(\text{H}_2\text{O})_2]$	$P\bar{1}$	15g
Childrenite	$\text{Mn}^{2+}[\text{Al}(\text{PO}_4)(\text{OH})_2(\text{H}_2\text{O})]$	$Bbam$	15b	Fairfieldite	$\text{Ca}_2[\text{Mn}(\text{PO}_4)_2(\text{H}_2\text{O})_2]$	$P\bar{1}$	15g
Eosphorite	$\text{Fe}^{2+}[\text{Al}(\text{PO}_4)(\text{OH})_2(\text{H}_2\text{O})]$	$Bbam$	15b	Messelite	$\text{Ca}_2[\text{Fe}^{2+}(\text{PO}_4)_2(\text{H}_2\text{O})_2]$	$P\bar{1}$	15g
Uklonskovite	$\text{Na}[\text{Mg}(\text{SO}_4)(\text{OH})(\text{H}_2\text{O})_2]$	$P2_1/m$	15b	Tancoite	$\text{Na}_2\text{LiH}[\text{Al}(\text{PO}_4)_2(\text{OH})]$	$Pbcb$	15h
Fibroferrite	$[\text{Fe}^{3+}(\text{SO}_4)(\text{OH})(\text{H}_2\text{O})_2](\text{H}_2\text{O})_4$	$R\bar{3}$	15c	Sideronatrite	$\text{Na}_2[\text{Fe}^{3+}(\text{SO}_4)_2(\text{OH})](\text{H}_2\text{O})_3$	$Pnn2$	15h
Chlorothionite	$\text{K}_2[\text{Cu}(\text{SO}_4)\text{Cl}_2]$	$Pnma$	15d	Jahnsite	$\text{CaMnMg}_2[\text{Fe}^{3+}(\text{PO}_4)_2(\text{OH})_2](\text{H}_2\text{O})_8$	$P2_1/a$	15h
Linarite	$\text{Pb}[\text{Cu}(\text{SO}_4)(\text{OH})_2]$	$P2_1/m$	15e	Whiteite	$\text{CaFe}^{2+}\text{Mg}_2[\text{Al}(\text{PO}_4)_2(\text{OH})_2](\text{H}_2\text{O})_8$	$P2_1/a$	15h
Schmiederite	$\text{Pb}_2[\text{Cu}_2(\text{SeO}_4)(\text{SeO}_4)(\text{OH})_4]$	$P2_1/m$	15e	Lun'okite	$\text{Mn}_2\text{Mg}_2[\text{Al}(\text{PO}_4)_2(\text{OH})_2](\text{H}_2\text{O})_8$	$Pbca$	15h
Amarantite	$[\text{Fe}_2^{3+}(\text{SO}_4)_2(\text{H}_2\text{O})_4](\text{H}_2\text{O})_3$	$P\bar{1}$	15f	Overite	$\text{Ca}_2\text{Mg}_2[\text{Al}(\text{PO}_4)_2(\text{OH})_2](\text{H}_2\text{O})_8$	$Pbca$	15h
Hohmannite	$[\text{Fe}_2^{3+}(\text{SO}_4)_2(\text{H}_2\text{O})_4](\text{H}_2\text{O})_4$	$P\bar{1}$	15f	Segelerite	$\text{Ca}_2\text{Mg}_2[\text{Fe}^{3+}(\text{PO}_4)_2(\text{OH})_2](\text{H}_2\text{O})_8$	$Pbca$	15h
Sahamalite	$*(\text{RE})_2[(\text{Mg}, \text{Fe})(\text{CO}_3)_4]$	$P2_1/a$	15l	Wilhelmvierlingite	$\text{Ca}_2\text{Mn}_2[\text{Fe}^{3+}(\text{PO}_4)_2(\text{OH})_2](\text{H}_2\text{O})_8$	$Pbca$	15h
Dresserite	$\text{Ba}[\text{Al}(\text{CO}_3)(\text{OH})_2](\text{H}_2\text{O})$	$Pbnn$	15o	Guildite	$\text{Cu}^{2+}[\text{Fe}^{3+}(\text{SO}_4)_2(\text{OH})](\text{H}_2\text{O})_4$	$P2_1/m$	15h
Dundasite	$\text{Pb}[\text{Al}(\text{CO}_3)(\text{OH})_2](\text{H}_2\text{O})$	$Pbnn$	15o	Yftsite	$\text{Y}_4[\text{Ti}(\text{SiO}_4)_2\text{O}](\text{F}, \text{OH})_6$	$Cmcm$	15h
Strontiodresserite	$(\text{Sr}, \text{Ca})[\text{Al}(\text{CO}_3)(\text{OH})_2](\text{H}_2\text{O})$	$Pbnn$	15o	Arsenbrackebuschite	$\text{Pb}_2[\text{Fe}^{2+}(\text{AsO}_4)_2(\text{H}_2\text{O})]$	$P2_1/m$	15i
Hydrodresserite	$\text{Ba}[\text{Al}(\text{CO}_3)(\text{OH})_2](\text{H}_2\text{O})_3$	$P\bar{1}$	15o	Arsentsumebite	$\text{Pb}_2[\text{Cu}(\text{SO}_4)(\text{AsO}_4)(\text{OH})]$	$P2_1/m$	15i
Dawsonite	$\text{Na}[\text{Al}(\text{CO}_3)(\text{OH})_2]$	$Imma$	15o	Brackebuschite	$\text{Pb}_2[\text{Mn}(\text{VO}_4)_2(\text{H}_2\text{O})]$	$P2_1/m$	15i
Artinite	$\text{Mg}_2[(\text{CO}_3)(\text{OH})_2](\text{H}_2\text{O})_3$	$C2/m$	21	Gamagarite	$\text{Ba}_2[(\text{Fe}^{3+}, \text{Mn})(\text{VO}_4)_2(\text{OH}, \text{H}_2\text{O})]$	$P2_1/m$	15i
Nesquehonite	$[\text{Mg}(\text{CO}_3)(\text{H}_2\text{O})_2] \cdot \text{H}_2\text{O}$	$P2_1/n$	15m	Goedkenite	$\text{Sr}_2[\text{Al}(\text{PO}_4)_2(\text{OH})]$	$P2_1/m$	15i
Chalconatronite	$\text{Na}_2[\text{Cu}(\text{CO}_3)_2(\text{H}_2\text{O})](\text{H}_2\text{O})_3$	$P2_1/n$	15n	Tsumebite	$\text{Pb}_2[\text{Cu}(\text{PO}_4)(\text{SO}_4)(\text{OH})]$	$P2_1/m$	15i
				Fornacite	$\text{Pb}_2[\text{Cu}(\text{AsO}_4)(\text{CrO}_4)(\text{OH})]$	$P2_1/c$	15i
				Molybdoformacite	$\text{Pb}_2[\text{Cu}(\text{AsO}_4)(\text{MoO}_4)(\text{OH})]$	$P2_1/c$	15i
				Tornebohmitite	$*(\text{RE})_2[\text{Al}(\text{SiO}_4)_2(\text{OH})]$	$P2_1/c$	15i
				Vauquelinite	$\text{Pb}_2[\text{Cu}(\text{PO}_4)(\text{CrO}_4)(\text{OH})]$	$P2_1/n$	15i
				Ransomite	$\text{Cu}[\text{Fe}^{3+}(\text{SO}_4)_2(\text{H}_2\text{O})_2](\text{H}_2\text{O})_4$	$P2_1/c$	15j
				Krausite	$\text{K}[\text{Fe}^{3+}(\text{SO}_4)_2(\text{H}_2\text{O})]$	$P2_1/m$	15j
				Botryogen	$\text{Mg}_2[\text{Fe}_2^{3+}(\text{SO}_4)_4(\text{OH})_2(\text{H}_2\text{O})_2](\text{H}_2\text{O})_{10}$	$P2_1/n$	15j
				Zincbotryogen	$\text{Zn}_2[\text{Fe}_2^{3+}(\text{SO}_4)_4(\text{OH})_2(\text{H}_2\text{O})_2](\text{H}_2\text{O})_{10}$	$P2_1/n$	15j

* RE = rare earth elements.

Infinite-chain structures

A large number of possible $[M_x(T\phi_4)_y\phi_z]$ and $[M_x(T\phi_3)_y\phi_z]$ chains can be constructed from fundamental building blocks involving one or two octahedra and one, two or four tetrahedra or triangles. Only a few of these possible chains have actually been found in inorganic oxysalt structures and a cross-section of these is shown in Fig. 15; selected structures based on these chains are listed in Table 5.

We may divide the chains of Fig. 15 into two types: *common* [(a), (b), (c), (g), (h), (i) and (l)] and *rare* [(d), (e), (f), (j), (k), (m), (n), (o) and (p)]. Structures based on these chains are listed in Table 5. Minerals based on common chains are much more abundant than minerals based on rare chains and also tend to show many more isostructural species than minerals based on rare chains.

Consider first the common chains of stoichiometry $[M(T\phi_4)\phi_n]$ [Figs. 15(a), (b) and (c)]. The first chain [Fig. 15(a)] has no linkage between octahedra, the second chain [Fig. 15(b)] has corner linkage between octahedra and the third chain [Fig. 15(c)] has edge linkage between octahedra. These are the more important of the chains in this group and it is notable that

(a) they all have a fairly simple connectivity;

(b) there is just one particular chain for each type of connectivity between octahedra; thus in the first chain, there is no direct linkage between octahedra; in the second chain, there is corner-sharing between octahedra; in the third chain, there is edge-sharing between octahedra.

Graph-theoretical arguments show that there are 200–300 distinct chains based on repeat units of $[M(T\phi_4)\phi_n]$ and $[M_2(T\phi_4)_2\phi_{2n}]$. Very few of these

Table 6. $M(T\phi_4)\phi_n$, $M(T\phi_4)_2\phi_n$ and $M_x(T\phi_3)_y\phi_z$ minerals based on infinite sheets of $M\phi_6$ octahedra, $T\phi_4$ tetrahedra and $T\phi_3$ triangles

$M(T\phi_4)\phi_n$ mineral	Formula	Space group	Fig.	$M(T\phi_4)_2\phi_n$ mineral	Formula	Space group	Fig.
Newberyite	$[\text{Mg}(\text{PO}_4\text{OH})(\text{H}_2\text{O})_3]$	<i>Pbca</i>	16a	Rhombochase	$(\text{H}_2\text{O})_2[\text{Fe}^{3+}(\text{SO}_4)_2(\text{H}_2\text{O})_2]$	<i>Pnma</i>	17a
Minyulite	$\text{K}[\text{Al}_2(\text{PO}_4)_2\text{F}(\text{H}_2\text{O})_4]$	<i>Pba2</i>	16b	Olmsteadite	$\text{KFe}_2^{3+}[\text{Nb}(\text{PO}_4)_2\text{O}_2](\text{H}_2\text{O})_2]$	<i>Pb2_1m</i>	17b
Gordonite	$\text{Mg}[\text{Al}_2(\text{PO}_4)_2(\text{OH})_2(\text{H}_2\text{O})_2](\text{H}_2\text{O})_4 \cdot 2(\text{H}_2\text{O})$	<i>P\bar{1}</i>	16c	Brianite	$\text{Na}_2\text{Ca}[\text{Mg}(\text{PO}_4)_2]$	<i>P2_1/a</i>	17c
Laueite	$\text{Mn}^{2+}[\text{Fe}_2^{3+}(\text{PO}_4)_2(\text{OH})_2(\text{H}_2\text{O})_2](\text{H}_2\text{O})_4 \cdot 2(\text{H}_2\text{O})$	<i>P\bar{1}</i>	16c	Merwinite	$\text{Ca}_3[\text{Mg}(\text{SiO}_4)_2]$	<i>P2_1/a</i>	17c
Paravauxite	$\text{Fe}^{2+}[\text{Al}_2(\text{PO}_4)_2(\text{OH})(\text{H}_2\text{O})_2](\text{H}_2\text{O})_4 \cdot 2(\text{H}_2\text{O})$	<i>P\bar{1}</i>	16c	Yavapaite	$\text{K}[\text{Fe}^{3+}(\text{SO}_4)_2]$	<i>C2/m</i>	17c
Sigloite	$(\text{Fe}^{3+}, \text{Fe}^{2+})[\text{Al}_2(\text{PO}_4)_2(\text{OH})_2(\text{H}_2\text{O})_2](\text{H}_2\text{O}, \text{OH})_4 \cdot 2(\text{H}_2\text{O})$	<i>P\bar{1}</i>	16c	Bafertisite	$\text{BaFe}^{2+}[\text{Ti}(\text{Si}_2\text{O}_7)_2\text{O}_2]$	<i>C2/m</i>	17d
Ushkovite	$\text{Mg}[\text{Fe}_2^{3+}(\text{PO}_4)_2(\text{OH})_2(\text{H}_2\text{O})_2](\text{H}_2\text{O})_4 \cdot 2(\text{H}_2\text{O})$	<i>P\bar{1}</i>	16c	Pyrophyllite	$[\text{AlSi}_2\text{O}_6(\text{OH})]$	<i>C\bar{1}</i>	—
Stewartite	$\text{Mn}^{2+}[\text{Fe}_2^{3+}(\text{PO}_4)_2(\text{OH})_2(\text{H}_2\text{O})_2](\text{H}_2\text{O})_4 \cdot 2(\text{H}_2\text{O})$	<i>P\bar{1}</i>	16e	Diocahedral micas	(M^+, M^{2+}) $[(M^{3+}, M^{2+})(\text{Si}, \text{Al})_2\text{O}_2(\text{OH})_2]$	<i>C2/m</i>	—
Pseudolaueite	$\text{Mn}^{2+}[\text{Fe}^{3+}(\text{PO}_4)(\text{OH})(\text{H}_2\text{O})_2](\text{H}_2\text{O})_4 \cdot 2(\text{H}_2\text{O})$	<i>P2_1/a</i>	16d	Ephesite	$\text{NaLi}[\text{Al}(\text{Si}, \text{Al})_2\text{O}_2(\text{OH})_2]$	<i>C2/m</i>	—
Strunzite	$\text{Mn}^{2+}[\text{Fe}^{3+}(\text{PO}_4)(\text{OH})(\text{H}_2\text{O})_2](\text{H}_2\text{O})_4$	<i>P\bar{1}</i>	—	Taenolite	$\text{KLi}[\text{MgSi}_2\text{O}_7(\text{OH})_2]$	<i>C2/m</i>	—
Ferrostrunzite	$\text{Fe}^{2+}[\text{Fe}^{3+}(\text{PO}_4)(\text{OH})(\text{H}_2\text{O})_2](\text{H}_2\text{O})_4$	<i>P\bar{1}</i>	—	Diocahedral smectites	$(M^+, \text{H}_2\text{O})$ $[(M^{3+}, M^{2+})(\text{Si}, \text{Al})_2\text{O}_2(\text{OH})_2]$	—	—
Metavauxite	$\text{Fe}^{2+}[\text{Al}(\text{PO}_4)(\text{OH})(\text{H}_2\text{O})_2](\text{H}_2\text{O})_4$	<i>P2_1/c</i>	15f	Bramallite	$(M^+, \text{H}_2\text{O})$ $[(\text{Al}, \text{Mg}, \text{Fe})(\text{Si}, \text{Al})_2\text{O}_2(\text{OH})_2]$	—	—
Tsumcorite	$\text{Pb}[(\text{Zn}, \text{Fe}^{3+})(\text{AsO}_4)(\text{H}_2\text{O}, \text{OH})_2]$	<i>C2/m</i>	15h	Hydromica	$(M^+, \text{H}_2\text{O})_2[\text{Al}(\text{Si}, \text{Al})_2\text{O}_2(\text{OH})_2]$	—	—
Bermanite	$\text{Mn}^{2+}[\text{Mn}^{3+}(\text{PO}_4)(\text{OH})_2](\text{H}_2\text{O})_4$	<i>P2_1</i>	15h	Illite	$(M^+, \text{H}_2\text{O})_2$ $[(\text{Al}, \text{Mg}, \text{Fe})(\text{Si}, \text{Al})_2\text{O}_2(\text{OH})_2]$	<i>C2/c</i>	—
Foggite	$\text{Ca}[\text{Al}(\text{PO}_4)(\text{OH})_2](\text{H}_2\text{O})$	<i>A2,22</i>	—	Goldichite	$\text{K}_2[\text{Fe}_2^{3+}(\text{SO}_4)_2(\text{H}_2\text{O})_4](\text{H}_2\text{O})_4$	<i>P2_1/c</i>	—
Arthurite	$\text{Cu}[\text{Fe}^{3+}(\text{AsO}_4)(\text{OH})_2](\text{H}_2\text{O})_4$	<i>P2_1/c</i>	15g	Buetschliite	$\text{K}_2[\text{Ca}(\text{CO}_3)_2]$	<i>R\bar{3}</i>	17e
Earlshannonite	$\text{Mn}^{2+}[\text{Fe}^{3+}(\text{PO}_4)(\text{OH})_2](\text{H}_2\text{O})_4$	<i>P2_1/c</i>	15g	Eitelite	$\text{Na}_3[\text{Mg}(\text{CO}_3)_2]$	<i>R\bar{3}</i>	17e
Ojuelaite	$\text{Zn}[\text{Fe}^{3+}(\text{AsO}_4)(\text{OH})_2](\text{H}_2\text{O})_4$	<i>P2_1/c</i>	15g	Tunisiaite	$\text{NaCa}_2\text{Cl}[\text{Al}_2(\text{CO}_3)_2(\text{OH})_4]$	<i>PA/nm</i>	17f
Whitmoreite	$\text{Fe}^{2+}[\text{Fe}^{3+}(\text{PO}_4)(\text{OH})_2](\text{H}_2\text{O})_4$	<i>P2_1/c</i>	15g	Rodaquilarite	$\text{H}_3\text{Cl}[(\text{Fe}_2^{3+}(\text{TeO}_3)_4)]$	<i>P\bar{1}</i>	17g
Krautite	$[\text{Mn}^{2+}(\text{AsO}_4)(\text{OH})(\text{H}_2\text{O})]$	<i>P2_1</i>	—	Denningite	$(\text{Ca}, \text{Mn})[(\text{Mn}, \text{Zn})(\text{Te}_2\text{O}_3)_2]$	<i>PA_2/n</i>	17h
Fluckite	$[\text{CaMn}^{2+}(\text{AsO}_4)(\text{OH})_2](\text{H}_2\text{O})_2]$	<i>P\bar{1}</i>	—				
Co-Koritnigite	$[\text{Co}(\text{AsO}_4)(\text{OH})(\text{H}_2\text{O})]$	<i>P\bar{1}</i>	—				
Koritnigite	$[\text{Zn}(\text{AsO}_4)(\text{OH})(\text{H}_2\text{O})]$	<i>P\bar{1}</i>	—				
Kaolinite	$[\text{Al}_2\text{Si}_2\text{O}_5(\text{OH})_4]$	<i>C1</i>	—				
Dickite	$[\text{Al}_2\text{Si}_2\text{O}_5(\text{OH})_4]$	<i>Cc</i>	—				
Nacrite	$[\text{Al}_2\text{Si}_2\text{O}_5(\text{OH})_4]$	<i>Cc</i>	—				
Arsenosiderite	$\text{Ca}_2[\text{Fe}_2^{3+}(\text{AsO}_4)_2\text{O}_2](\text{H}_2\text{O})_3]$	<i>Aa</i>	—				
Kolfanite	$\text{Ca}_2[\text{Fe}_2^{3+}(\text{AsO}_4)_2\text{O}_2](\text{H}_2\text{O})_2]$	<i>Aa</i>	—				
Mitridatite	$\text{Ca}_2[\text{Fe}_2^{3+}(\text{PO}_4)_2\text{O}_2](\text{H}_2\text{O})_3]$	<i>Aa</i>	—				
Robertsite	$\text{Ca}_2[\text{Mn}_2^{3+}(\text{PO}_4)_2\text{O}_2](\text{H}_2\text{O})_3]$	<i>Aa</i>	—				

are found in structures and by far the most common chains are the three simplest chains in which the octahedra share none, and one and two anions, respectively.

Consider next the common chains of stoichiometry $[M(T\phi_4)_2\phi_n]$ [Figs. 15(g), (h) and (i)]. Again, these chains have no linkage, corner linkage and edge linkage, respectively, between adjacent octahedra and are the three simplest possible chains of $[M(T\phi_4)_2\phi_n]$ stoichiometry. The parallel behavior of the $[M(T\phi_4)\phi_n]$ and $[M(T\phi_4)_2\phi_n]$ chain structures is striking, to say the least. The more complex chains of Figs. 15(d), (e) and (f) are found in a smaller number of (far less common) minerals. In addition, it seems that the more complex structural units tend to occur in the ferric-iron sulphates.

There are far fewer chain-structures in the $[M_x(T\phi_3)_y\phi_z]$ minerals (Table 5) and it should be noted that the stoichiometry of these structures is less constrained than for the $[M(T\phi_4)\phi_n]$ and $[M(T\phi_4)_2\phi_n]$ groups. Nevertheless, a similar type of pattern is seen among the simpler structural units.

There is one chain [Fig. 15(l)] with no linkage between octahedra, two chains [Figs. 15(m) and (n)] with corner linkage between octahedra and one chain [Fig. 15(o)] with edge linkage between octahedra, plus one more complex chain [Fig. 15(p)]. Thus, again, the same pattern seems apparent, despite the fact that the corner-linking octahedral chains have the added complication that the (carbonate) triangle shares an edge with the octahedron.

Infinite-sheet structures

Minerals of this class are given in Table 6. As the degree of polymerization of the structural unit increases, the number of possible bond connectivities becomes enormous. However, nature still seems to favor only a fairly small number of them; these are illustrated in Figs. 16 and 17.

There is far more variety in the sheet structures of the $M(T\phi_4)\phi_n$ minerals. Notable in the less-connected structural units is that of minyulite [Fig. 16(b)], which is built by condensation (*via* corner

linkage between octahedra and tetrahedra) of $[M_2(T\phi_4)_2\phi_7]$ clusters (Kampf, 1977) that are the structural unit in morinite [Fig. 13(c)]. The structures of laueite, stewartite, pseudolaueite, strunzite and metavauxite groups [Figs. 16(c)–(f)] are based on sheets formed from condensation of the vertex-sharing octahedral–tetrahedral chains of the sort shown in Figs. 15(b) and (h). The tetrahedra cross-link the chains into sheets and there is much possible variation in this type of linkage; for more details on this isomerism, see Moore (1975). The five structural groups of these minerals are based on the four sheets of Figs. 16(c)–(f). These sheets are linked through insular divalent metal octahedra, either by direct corner-linkage to phosphate tetrahedra plus hydrogen bonding or by hydrogen bonding alone. There is great potential for stereoisomerism in the ligand arrangement of these linking octahedra, but only the *trans*-corner linkages occur in these groups. In the whitmoreite sheet (Moore, Kampf & Irving, 1974) [Fig. 16(g)], we can see both the $[M_2(T\phi_4)_2\phi_7]$ cluster of the morinite structure and the $[M_2(T\phi_4)_2\phi_8]$ cluster of the rozenite group structures [Figs. 13(c) and (b)]. Similarly, in the $[M(T\phi_4)\phi]$ sheet of the bermanite (Kampf & Moore, 1976) and tsumcorite (Tillmanns & Gebert, 1973) structures [Fig. 16(h)], we can see the $[M(T\phi_4)\phi_2]$ chain that is the struc-

tural unit in the minerals of the linarite group [Fig. 15(e)].

The sheet units found in the $M(T\phi_4)_2\phi_n$ and $M_x(T\phi_3)_y\phi_n$ minerals are shown in Fig. 17. Again we see this structural building process, whereby structural units of more primitive connectivities act as fundamental building blocks for the more condensed structural units of corresponding composition. Thus, the $[M(T\phi_4)_2\phi_2]$ sheet in rhomboclase (Mereiter, 1974) [Fig. 17(a)] is constructed from the *cis*- $[M(T\phi_4)_2\phi_4]$ cluster that is the structural unit of roemerite [Fig. 13(d)]. Similarly, the $[M(T\phi_4)_2\phi_2]$ sheet of olmsteadite (Moore, Araki, Kampf & Steele, 1976) [Fig. 17(b)] is based on the *trans*- $[M(T\phi_4)_2\phi_4]$ cluster [Fig. 13(e)] found in anapaite, bloedite, leonite and schertelite [Figs. 14(c)–(f)]. Note that the rhomboclase and olmsteadite sheets are actually *geometrical isomers* (Hawthorne, 1983). Analogous relationships are obvious for the $[M(T\phi_4)_2]$ merwinite-type sheet and the $[M(T_2\phi_7)\phi_2]$ bafertisite-type sheet [Figs. 17(c) and (d)]. Both are based on the $[M(T\phi_4)_2\phi_2]$ krohnkite chain of Fig. 15(g), but in each sheet, the chains are cross-linked in a different fashion. In the merwinite sheet (Moore & Araki, 1972), tetrahedra from one chain share corners with octahedra of adjacent chains and neighboring tetrahedra point in opposite directions

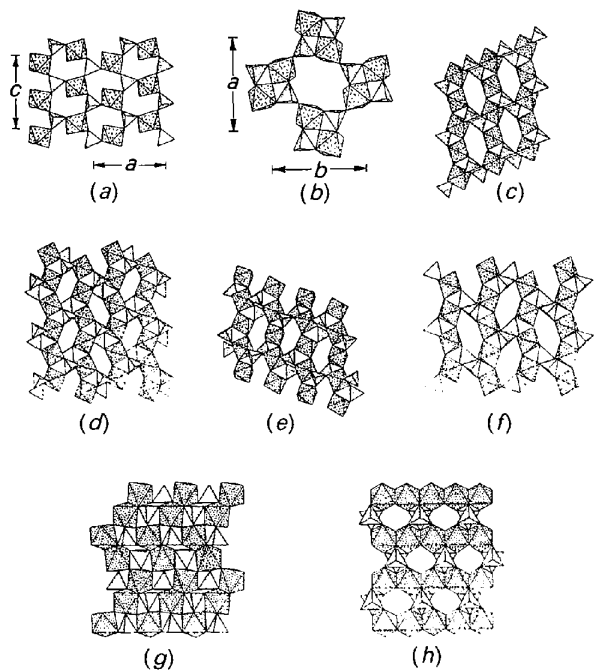


Fig. 16. Selected infinite sheets in $[M(T\phi_4)\phi_n]$ structures: (a) the $[M(T\phi_4)\phi_3]$ sheet in newberyite; (b) the $[M_2(T\phi_4)_2\phi_5]$ sheet in minyulite; (c) the $[M(T\phi_4)\phi_2]$ sheet in the laueite-group minerals; (d) the $[M(T\phi_4)\phi_2]$ sheet in pseudolaueite; (e) the $[M(T\phi_4)\phi_2]$ sheet in stewartite; (f) the $[M(T\phi_4)\phi_2]$ sheet in metavauxite; (g) the $[M_2(T\phi_4)_2\phi_7]$ sheet in whitmoreite; (h) the $[M(T\phi_4)\phi]$ sheet in tsumcorite and bermanite.

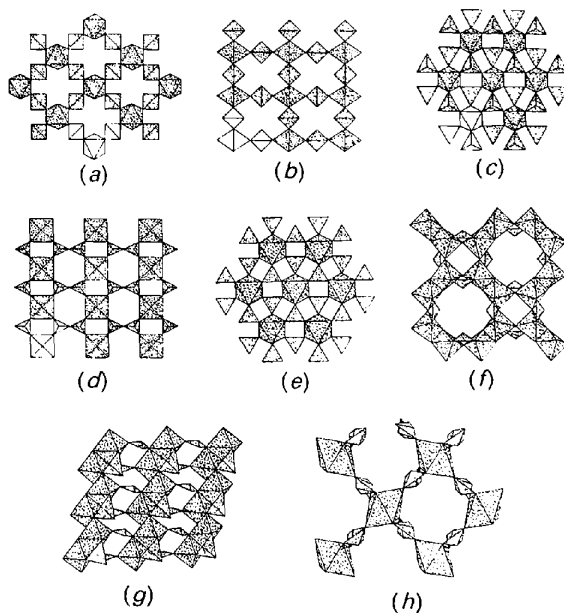


Fig. 17. Selected infinite sheets in $[M(T\phi_4)_2\phi_n]$ and $[M_x(T\phi_3)_y\phi_n]$ structures: (a) the $[M(T\phi_4)_2\phi_2]$ sheet in rhomboclase; (b) the $[M(T\phi_4)_2\phi_2]$ sheet in olmsteadite; (c) the $[M(T\phi_4)_2]$ sheet in the merwinite-group minerals and yavapaite; (d) the $[M(T_2\phi_7)\phi_2]$ sheet in bafertisite; (e) the $[M(T\phi_3)_2]$ sheet in the eitelite-group minerals; (f) the $[M(T\phi_3)\phi_2]$ sheet in tunisite; (g) the $[M_2(T\phi_3)_2\phi_4]$ sheet in rodalquilarite; (h) the $[M(T_2\phi_5)_2]$ sheet in denningite.

relative to the plane of the sheet. In the bafertisite sheet (Ya-Hsien, Simonov & Belov, 1963), the $[M(T\phi_4)_2\phi_2]$ chains link by sharing corners between tetrahedra. Thus, both sheets are 'built' from the same more primitive structural unit and these two sheets are in fact *graphical isomers* (Hawthorne, 1983).

Framework structures

Selected minerals of this class are listed in Table 7. Unfortunately, the topological aspects of the framework structures cannot be easily summarized in a concise graphical fashion, partly because of their large number and partly because of the complexity that results from polymerization in all three spatial dimensions. Consequently, we will consider just a few examples that show particularly clearly the different types of linkages that can occur.

The structure of bonattite (Zahrobsky & Baur, 1968) is shown in Fig. 18(a). Bonattite is quite hydrated (Table 7) and comparison with the minerals of Table 6 suggests that it should be a sheet structure (*c.f.* newberyite, Table 6). Prominent in the structure are the $[M(T\phi_4)\phi_4]$ chains [Fig. 14(a)] that also occur as fragments of the newberyite sheet [Fig. 16(a)]. In bonattite, adjacent chains are skew and link to form a framework; in newberyite (Sutor, 1967), the chains are parallel, and with the same number of inter-chain linkages, they link to form sheets rather than a framework. Thus, bonattite and newberyite are *graphical isomers* and provide a good illustration of how different modes of linking the same fundamental building block can lead to structures of very different connectivities and properties.

The structure of titanite is shown in Fig. 18(b); this basic arrangement is found in a considerable number of minerals (Table 7) of widely differing chemistry (Hawthorne, Groat, Raudsepp & Ercit, 1987). The $[M(T\phi_4)\phi]$ framework can be constructed from $[M(T\phi_4)\phi]$ vertex-sharing chains of the sort found in butlerite (Fanfani, Nunzi & Zanazzi, 1971), parabutlerite (Borene, 1970), the childrenite group

Table 7. $M(T\phi_4)\phi_n$ minerals based on infinite frameworks of $M\phi_4$ octahedra, $T\phi_4$ tetrahedra and $T\phi_3$ triangles

$M(T\phi_4)\phi_n$ mineral	Formula	Space group	Fig.
Bonattite	$[\text{Cu}(\text{SO}_4)(\text{H}_2\text{O})_3]$	Cc	18a
Amblygonite	$\text{Li}[\text{Al}(\text{PO}_4)\text{F}]$	$C\bar{1}$	18b
Montebrasite	$\text{Li}[\text{Al}(\text{PO}_4)\text{OH}]$	$C\bar{1}$	18b
Tavorite	$\text{Li}[\text{Fe}^{2+}(\text{PO}_4)\text{OH}]$	$C\bar{1}$	18b
Arsendescloizite	$\text{Pb}[\text{Zn}(\text{AsO}_4)\text{OH}]$	$Pnam$	18c
Calciovolborthite	$\text{Ca}[\text{Cu}(\text{VO}_4)\text{OH}]$	$Pnam$	18c
Cechite	$\text{Pb}[\text{Fe}^{2+}(\text{VO}_4)\text{OH}]$	$Pnam$	18c
Descloizite	$\text{Pb}[\text{Zn}(\text{VO}_4)\text{OH}]$	$Pnam$	18c
Mottamite	$\text{Pb}[\text{Cu}(\text{VO}_4)\text{OH}]$	$Pnam$	18c
Pyrobelonite	$\text{Pb}[\text{Mn}(\text{VO}_4)\text{OH}]$	$Pnam$	18c
Durangite	$\text{Na}[\text{Al}(\text{AsO}_4)\text{F}]$	Cc	18b
Isokite	$\text{Ca}[\text{Mg}(\text{PO}_4)\text{F}]$	$C2/c$	18b
Lacroixite	$\text{Na}[\text{Al}(\text{PO}_4)\text{F}]$	$C2/c$	18b
Malayaite	$\text{Ca}[\text{Sn}^{2+}(\text{SiO}_4)\text{O}]$	$C2/c$	18b
Panasquereite	$\text{Ca}[\text{Mg}(\text{PO}_4)\text{OH}]$	$C2/c$	18b
Tilasite	$\text{Ca}[\text{Mg}(\text{AsO}_4)\text{F}]$	Cc	18b
Titanite- $P2_1/c$	$\text{Ca}[\text{Ti}(\text{SiO}_4)\text{O}]$	$P2_1/c$	18b
Titanite- $C2/c$	$\text{Ca}[(\text{Ti}, \text{Al}, \text{Fe})(\text{SiO}_4)\text{O}]$	$C2/c$	18b
Dwornikite	$[\text{Ni}(\text{SO}_4)(\text{H}_2\text{O})]$	$C2/c$	18b
Gunningite	$[\text{Zn}(\text{SO}_4)(\text{H}_2\text{O})]$	$C2/c$	18b
Kieserite	$[\text{Mg}(\text{SO}_4)(\text{H}_2\text{O})]$	$C2/c$	18b
Poitevinite	$[\text{Cu}(\text{SO}_4)(\text{H}_2\text{O})]$	$C2/c$	18b
Szmikite	$[\text{Mn}^{2+}(\text{SO}_4)(\text{H}_2\text{O})]$	$C2/c$	18b
Szolmonokite	$[\text{Fe}^{2+}(\text{SO}_4)(\text{H}_2\text{O})]$	$C2/c$	18b

(Giuseppetti & Tadini, 1984) and uklonskovite (Sabelli, 1985b) [Table 5, Fig. 15(b)]. The chains pack in a C-centered array and cross-link by sharing corners between octahedra and tetrahedra of adjacent chains. It is notable that this chain is also a fundamental building block of the sheets [Figs. 16(c)–(f)] in the laueite, stewartite, pseudolaueite, strunzite and metavauxite groups (Table 6).

The structure of descloizite (Hawthorne & Fagiani, 1979) is shown in Fig. 18(c); again this is a popular structural arrangement (Table 7). Prominent features of the tetrahedral–octahedral framework are the edge-sharing chains of octahedra flanked by staggered tetrahedra that link along the chain. This $[M(T\phi_4)\phi]$ chain is found in the structures of the linarite-group minerals [Fig. 14(c)] and is also a fundamental building block for the $[M(T\phi_4)\phi]$ sheet [Fig. 15(e)] that is the structural unit in tsumcorite and bermanite (Table 6).

These three examples show the type of structural variability we find in the framework structures and also the small number of polyhedral linkage patterns (fundamental building blocks) that occur and seem common to a wide range of structural types. This suggests that these patterns of bond connectivity are very stable and hence tend to persist from one structure type to another. In addition, the incorporation of relatively primitive fragments into more highly condensed structural units tends to support the conceptual approach of considering a large structure both topologically and energetically as an assemblage of smaller structural fragments.

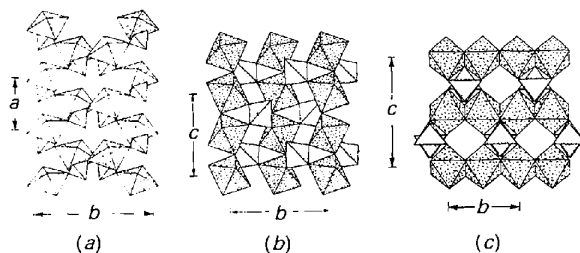


Fig. 18. Selected framework structures in $[M(T\phi_4)\phi_n]$ and $[M(T\phi_4)_2\phi_n]$ minerals: (a) the $[M(T\phi_4)\phi_3]$ framework structure of bonattite; (b) the $[M(T\phi_4)\phi]$ framework structure of titanite; (c) the $[M(T\phi_4)\phi]$ framework structure of descloizite.

(OH) and (H₂O) in oxysalt structures

One thing that emerges from the above discussion of structural hierarchy is the importance of hydrogen. It is not just in organic and biological structures that hydrogen is important. Because of its unusual stereochemical propensities, it has a unique role in controlling or moderating many aspects of structure and properties in inorganic crystals.

The hydrogen cation H⁺ commonly has a coordination number of 2 in inorganic structures; higher coordination numbers are not rare, but for simplicity we will consider the former, as the arguments presented here can easily be generalized to higher coordination numbers. There is usually a spontaneous distortion, with the hydrogen ion moving off-center towards one of the two coordinating anions. The geometry of this arrangement has been well-characterized by neutron diffraction (Ferraris & Franchini-Angela, 1972); the typical arrangement is shown in Fig. 18. Brown (1976) has shown that the most common bond-valence distribution is about 0.80 v.u. to the closer O atom and approximately 0.20 v.u. to the further O atom. This generally leads to the stronger bond being included in (H₂O)[°] or (OH)⁻ groups that now become complex anions; the longer (weaker) bond is referred to as a *hydrogen bond*. The O atom closest to the H atom is called the (hydrogen-bond) *donor* and the O atom further from the H atom is called the (hydrogen-bond) *acceptor* (Fig. 18).

There are six distinct hydrogen-bearing groups in inorganic structures: (OH)⁻, (H₂O)[°], (H₃O)⁺, (H₃O₂)⁻, (H₅O₂)⁺ and (NH₄)⁺; sketches of typical bond-valence distributions for these groups in minerals are shown in Fig. 20. The positively charged groups act as cations and both (H₃O)⁺ and (H₅O₂)⁺ are uncommon; typical examples are {H₃O}[Fe₂²⁺(SO₄)(OH)₆] (Ripmeester, Ratcliffe, Dutrizac & Jambor, 1986) and {H₅O₂}[Fe³⁺(SO₄)₂(H₂O)₂] (Mereiter, 1974). On the other hand, the (OH)⁻ and (H₂O)[°] groups play a very important role in oxysalt structures, particularly with regard to the topological properties of their bond networks. The reason for this stems from the extremely polar nature of these

two groups. On the oxygen side of each group, they function as an anion, whereas on the hydrogen side of each group, they function as a cation (Fig. 19); it is because of this unusual property that they play such a unique role in controlling the structure and chemistry of oxysalts.

Other large H...O groupings have been noted [e.g. (H₇O₃)⁺ in (H₇O₃)[C₆H₃Cl₂SO₃] and (H₁₄O₆)²⁺ in HSB₂Cl₆·3H₂O (Emsley, Jones & Lucas, 1981)]. However, these larger groups can be considered as smaller tightly bonded (*i.e.* D—H groups) groups linked by much weaker H...A bonds and thus I do not consider them as integral units; they are intermediate between the integral units noted above [*i.e.* (OH)⁻, (H₂O)[°], (H₃O)⁺ and (H₅O₂)⁻] and clathrate structures.

(OH) and (H₂O) as components of the structural unit

The polar character of these two groups (Fig. 20) allows them to control the character of the structural unit. On the Lewis-base side of each group, the bond valence is relatively strong, approximately 1.2 v.u. for (OH) and 0.4 v.u. for (H₂O); the remainder of the bond-valence requirements of the central O atom is satisfied by the H atom(s). On the Lewis-acid side of the group, the bond valence is relatively weak, about 0.2 v.u. for each group (Fig. 20). Thus, on the Lewis-base (or anionic) side of the group, the strong bond constitutes part of the bonding network of the structural unit; conversely, on the Lewis-acid (or cationic) side of the group, the hydrogen bond is too weak to form part of the bonding network of the structural unit. Hence, *the role of both (OH) and (H₂O) is to prevent the polymerization of the structural unit in specific directions*. Consequently, these groups play a crucial role in controlling the class of polymerization of the structural unit (Hawthorne, 1992).

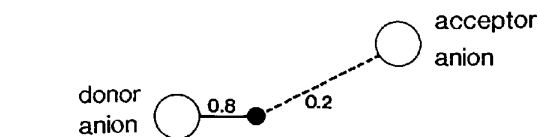


Fig. 19. Typical geometry of hydrogen coordination: the hydrogen is two-coordinate and spontaneously moves off-center to form two bonds of the approximate valence shown, and a bent O—H—O angle; the anion closer to the H atom is called the 'donor' anion and the anion furthest from the H atom is called the 'acceptor' anion.

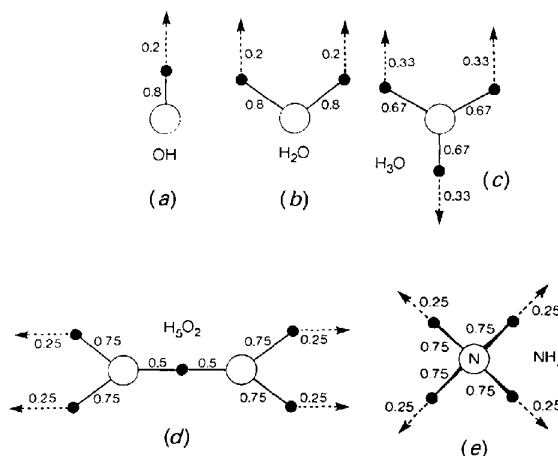


Fig. 20. Typical bond-valence distributions for the hydrogen-bearing groups found in the minerals: (a) (OH)⁻; (b) (H₂O)[°]; (c) (H₃O)⁺; (d) (H₅O₂)⁺; (e) (NH₄)⁺.

Table 8. *Bond-valence table for newberyite*

	Mg	P	H(6)	H(71)	H(72)	H(81)	H(82)	H(91)	H(92)	Sum
O(3)	0.389	1.399								1.788
O(4)	0.349	1.242	0.20	0.20						1.891
O(5)	0.364	1.232			0.20	0.20				1.996
O(6)		1.095	0.80				0.20			2.095
O(7)	0.326			0.80	0.80			0.20		2.126
O(8)	0.316					0.80	0.80		0.20	2.116
O(9)	0.313							0.80	0.80	1.913
Sum	2.057	4.968	1.0	1.0	1.0	1.0	1.0	1.0	1.0	

Newberyite (Sutor, 1967), $[\text{Mg}(\text{PO}_3\text{OH})(\text{H}_2\text{O})_3]$, illustrates this feature very well. The structural unit is a sheet of corner-sharing (MgO_6) octahedra and (PO_4) tetrahedra, with the polyhedra arranged at the vertices of a 6^3 net [Fig. 16(a)]; the bond-valence structure is shown in Table 8. In the (PO_4) tetrahedra, three of the ligands link to (MgO_6) octahedra within the sheet. The other ligand is 'tied off' orthogonal to the sheet by the fact that the O atom is strongly bonded to a H atom (*i.e.* it is an hydroxyl group). The long P—O bond of 1.59 Å contributes a bond valence of 1.10 v.u. to the O atom and the remaining 0.90 v.u. is contributed by the H atom, which then weakly hydrogen bonds (bond valence of about 0.10 v.u.) to the neighboring sheet in the y direction. In the (MgO_6) octahedra, three of the ligands link to (PO_4) tetrahedra within the sheets. The other ligands are 'tied off' by the fact that they are (H_2O) groups; the Mg—O bonds of 2.11, 2.12 and 2.13 Å contribute a bond valence of approximately 0.32 v.u. to each O atom and the remaining 1.68 v.u. is contributed by the two H atoms which then weakly hydrogen bond (~ 0.16 v.u. for each bond) to the neighboring sheets in the y direction. The chemical formula of the structural unit is also the chemical formula of the mineral and the sheet-like nature of the structural unit is controlled by the number and distribution of H atoms in the structure.

In newberyite, all intra-unit linkage stops at the (OH) and (H_2O) groups. This is not necessarily the case; both (OH) and (H_2O) can allow intra-unit linkage in some directions and prevent it in others. A good example of this is artinite, $[\text{Mg}_2(\text{CO}_3)(\text{OH})_2(\text{H}_2\text{O})_3]$ [(Akao & Iwai, 1977), Fig. 21 and Table 9]. The structural unit is a ribbon (chain) of edge-sharing (MgO_6) octahedra, flanked by (CO_3) triangles linked to alternate outer octahedral vertices of the ribbon in a staggered arrangement on either side of the ribbon. The anions down the centre of the ribbon are bonded to three Mg cations; they receive about $0.36 \times 3 = 1.08$ v.u. from the Mg cations and thus receive 0.92 v.u. from their associated H atoms, which then weakly hydrogen bond (bond valence approximately 0.08 v.u.) to an adjacent ribbon. The (OH) group thus *allows* linkage in the x and y

Table 9. *Bond-valence table for artinite*

	Mg	C	H(1)	H(2)	H(3)	H(4)	Sum
O(1)*	0.391		0.08			$0.80 \times 2 \rightarrow$	2.071
O(1')*	0.391	1.678	0.08				2.149
O(2)		$1.264 \times 2 \downarrow$		0.30	0.30		1.864
OH	$0.372 \times 2 \rightarrow$		0.92				2.014
	0.350						
OW	$0.283 \times 2 \downarrow \rightarrow$			0.70	0.70		1.966
	2.051	4.206	1.00	1.00	1.00	1.00	

*O(1) and O(1') are disordered and are both half-occupied.

directions, but *prevents* linkage in the z direction. The anions bonded to Mg along the edge of the ribbon are bonded to either one Mg, two Mg or one Mg and one C, with incident bond-valence contributions of 0.3, 0.6, and 1.7 v.u., respectively. The former two ligands must be (H_2O) groups which hydrogen bond fairly strongly to anions in the same and in adjacent structural units. Thus, the (H_2O) group bonded to one Mg prevents further unit polymerization in all three directions, whereas the (H_2O) group bonded to two Mg atoms allows polymerization in the y direction but prevents polymerization in the other two directions. The bond-valence requirements of the two anions bonded only to C are satisfied by hydrogen bonding involving donor atoms both in the same structural unit and in different structural units. Thus, in artinite, all linkage between structural units is through hydrogen

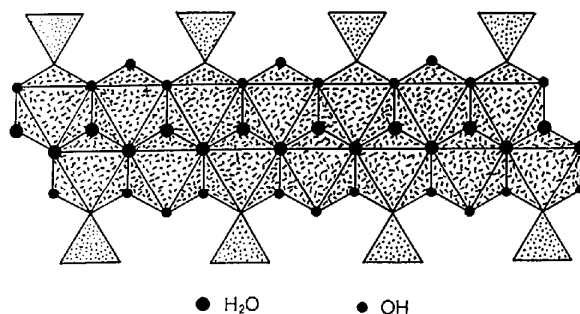


Fig. 21. The structural unit in artinite, a ribbon of (MgO_6) octahedra and (CO_3) triangles; all simple anions not bonded to carbon are either (OH) or (H_2O) .

bonding via (OH) and (H₂O) groups of the structural units. In addition, the (OH) groups allow polymerization in two directions within the structural unit, whereas the two types of (H₂O) groups allow polymerization in one and no directions, respectively, within the structural unit.

Hydroxyl and (H₂O) groups play an important role in the polymerization of the structural unit in oxysalt structures. Because of its very asymmetric distribution of bond valences, the H atom can link to any strongly bonded unit, essentially preventing any further polymerization in that direction. Thus, *the dimensionality of the structural unit is controlled primarily by the amount and role of hydrogen in the structure.*

(H₂O) groups bonded to interstitial cations

By definition (Lima de Faria, Hellner, Liebau, Makovicky & Parthé, 1990), interstitial cations are usually large and of low charge; they are usually alkali or alkaline-earth cations with Lewis acidities significantly less than the cations belonging to the structural unit. Consequently, (H₂O) can function as a ligand for these cations, whereas (OH) usually cannot, as the cation to which it must bond cannot contribute enough bond valence (*i.e.* about 1.0 v.u.) for its bond-valence requirements to be satisfied. There are (at least) three possible reasons for (H₂O) groups to act as ligands for interstitial cations:

(a) to satisfy the bond-valence requirements around the interstitial cation in cases where there are insufficient anions available from adjacent structural units;

(b) to carry the bond-valence from the interstitial cation to a distant unsatisfied anion of an adjacent structural unit;

(c) to act as a bond-valence transformer between the interstitial cation and the anions of the structural

unit; this is a mechanism of particular importance and will be discussed later.

An example of (H₂O) of this type occurs in stringhamite (Hawthorne, 1985b) [CaCu(SiO₄)](H₂O) (Fig. 22). The structural unit is a sheet of corner-sharing (SiO₄) tetrahedra and square-planar (CuO₄) polyhedra, arranged parallel to (010). These sheets are linked together by interstitial Ca atoms; each Ca links to four anions from one sheet and one anion from the adjacent sheet. Presumably, the Ca coordination number 5, a value which is rare for Ca, is not adequate with regard to the satisfaction of local bond-valence requirements, and two (H₂O) groups complete the Ca coordination polyhedron. Each (H₂O) group bonds to two Ca atoms (Fig. 22) and also hydrogen bonds to anions in adjacent sheets, carrying the Ca bond valence to anions which otherwise it could not reach. Thus, the (H₂O) groups of this type (*i.e.* bonded only to interstitial cations) play a very different role from those (H₂O) groups that form part of the structural unit.

Hydrogen-bonded interstitial (H₂O) groups

There are many structures in which interstitial (H₂O) groups are not bonded to any interstitial cations and yet occupy well defined positions within a structure and participate in a hydrogen-bonding network. The (H₂O) groups of this sort act as both hydrogen-bond donors and hydrogen-bond acceptors. Any hydrogen-containing group [both (OH) and (H₂O) of the structural unit, interstitial (H₂O) bonded to interstitial cations and interstitial (H₂O) groups not bonded to the structural unit or interstitial cations] can act as a hydrogen-bond donor to (H₂O) groups of this sort, and any anion or (H₂O) group can act as a hydrogen-bond acceptor

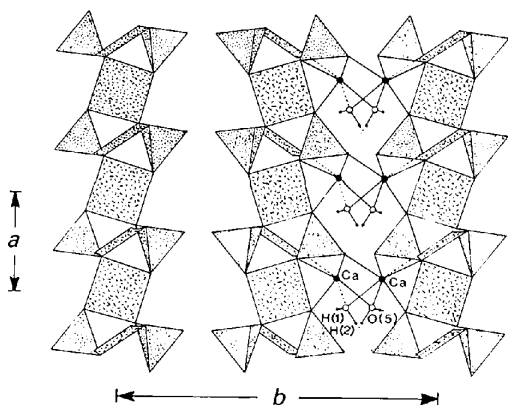


Fig. 22. The crystal structure of stringhamite projected on to (001); interstitial species are omitted on the left of the figure to emphasize the sheet-like nature of the structural unit.

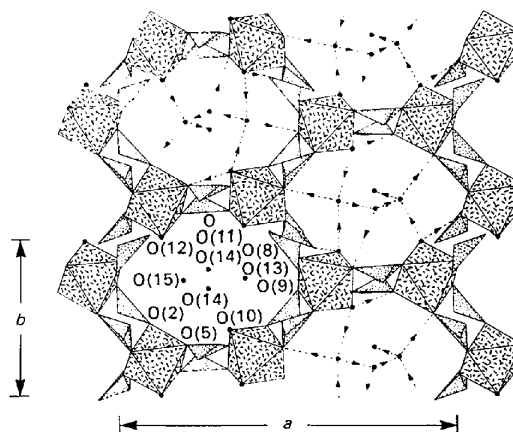


Fig. 23. The crystal structure of mandarinioite projected on to (001); note the two different types of (H₂O) groups, one bonded to cations of the structural unit and the other held in the structure by hydrogen-bonding only.

for such (H₂O) groups. Crystals with such hydrogen-bonding networks can be thought of as intermediate between anhydrous structures and clathrate structures. The clathrate-like fragments that constitute these hydrogen-bonded networks have been designated as large examples of H—O groups (Emsley, Jones & Lucas, 1981). However, for the reasons cited above, I consider them not as single groups but as part of the interstitial structure.

The structure of mandarinoite, [Fe₂³⁺(SeO₃)₃(H₂O)₃](H₂O)₃, shows such interstitial (H₂O) groups (Hawthorne, 1984*b*). The structural unit is a heteropolyhedral framework of corner-linked (SeO₃) triangular pyramids and (FeO₆) octahedra, with large cavities that are occupied by hydrogen-bonded (H₂O) groups in well defined positions (Fig. 23). Thus, of the six (H₂O) groups in the formula unit, three are bonded to Fe³⁺ and are part of the structural unit; the three remaining (H₂O) groups are interstitial and not bonded to any cation at all, but are held in place solely by a network of hydrogen bonds.

Occluded (H₂O) groups

Occluded (H₂O) groups are not bonded to any cation and are not associated with any hydrogen-bonding scheme; normally, such (H₂O) groups are located in holes within or between structural units. Such groups can occupy well defined crystallographic positions, but their linkage with the rest of the structure is solely through van der Waals' interaction.

Alkali-free beryl can have nonbonded (H₂O) groups occurring in the channels of the framework structure (Gibbs, Breck & Meagher, 1968). Most beryl contains alkali cations partly occupying sites within the channels and these cations are bonded to channel (H₂O) groups. However, Hawthorne & Cerny (1977) have shown that most beryl contains (H₂O) groups in excess of that required to coordinate the channel cations, and hence some of the (H₂O) groups must be occluded rather than occurring as bonded components of the structure. Although such (H₂O) does not play a significant structural role, it can have important effects on such physical properties as specific gravity, refractive indices (Cerny & Hawthorne, 1976) and dielectric behavior (Shannon, Subramanian, Mariano, Gier & Rossman, 1992).

Structure and chemical predictions

Thus far, we have been dealing with an *a posteriori* analysis: consideration of bond-valence theory as an MO theory, development of an hierarchical ordering of oxysalt structures, analysis of the various roles of hydrogen in oxysalt crystals. However, what we

really need to do is to develop some kind of predictive capability for aspects of structure and chemistry that have so far resisted our efforts. Bond-valence theory has a major role to play in this regard as it has predictive capability; we can use the Lewis acid and base values, together with the valence-matching principle, to examine possible chemical interactions without requiring detailed structural information. By using this approach, we can begin to examine several aspects of structure and chemistry that have hitherto resisted our efforts.

Binary structural representation

One of the problems in dealing with inorganic structures is the complexity of the atom interactions; there are a large number of them and their spatial characteristics are important. However, the same situation applies to an atom: there is a nucleus and numerous electrons, all interacting in a very complex manner; nevertheless, we can still usefully consider an atom as a single unit with simple properties such as size, charge and electronegativity. Why not take the same approach to the structural unit – consider it as a very complex oxyanion with intrinsic characteristic properties? When this is done (*e.g.* Hawthorne, 1985*a*, 1986, 1990), we can define a Lewis basicity for the structural unit in exactly the same manner as for a more conventional oxyanion.

Next, let us consider the interstitial components. These may be cations (*e.g.* alkalis or alkaline earths) and (H₂O) groups. As discussed above, (H₂O) groups may bond to interstitial cations; we may consider these as *complex cations* (*e.g.* [Ca(H₂O)₇]²⁺ groups), which then have properties (*e.g.* Lewis acidities) very different from their constituent simple cations. The interstitial components of a structure can usually be considered in a simple additive fashion to produce an aggregate set of properties (*e.g.* charge, Lewis acidity).

We have essentially factored the structure into two components and this enables us to use the valence-matching principle to examine the interaction of the structural unit with the interstitial species. It is worth emphasizing here that we have developed a *binary representation* that gives us a simple quantitative model of even the most complicated structure and allows us quantitative insight into the weak bonding between interstitial species and the structural unit.

This may be illustrated with goedkenite (Moore, Irving & Kampf, 1975), Sr₂[Al(PO₄)₂(OH)], the bond network of which is shown in Fig. 24. There are nine O atoms in this fragment (as indicated by the general [M(*Tφ*)_{2φ}] form of the structural unit) and the residual anionic charge is 4⁻. In order to calculate the basicity of this structural unit, we must assign the simple anion coordination numbers to the unit.

Obviously, there must be an objective process for doing this, as the calculation of structural unit basicity hinges on this assignment. Fortunately, this assignment is fairly well constrained by the general observation that most oxysalts of interest have O in three- or four-coordination; of course, it is easy to think of exceptions, quartz (SiO_2) for example, but the fact that these exceptions are few 'proves the rule'. Normally, it is adequate to use the coordination number 4; however, there are the following exceptions: (i) compounds with $M = 3^+$ and $T = 6^+$, for which the coordination number 3 is more appropriate; (ii) a coordination number of 3 (including H atoms) is more appropriate for (H_2O) , and is also used for (OH) when it is bonded to M^{3+} cations. To attain an O coordination number of 4, the cluster shown in Fig. 24 needs an additional number of bonds from the interstitial cations. From the connectivity of the structural unit, the cluster of Fig. 24 needs an additional 20 bonds; however, it will receive one (hydrogen) bond from an adjacent chain, which leaves 19 bonds to be received from the interstitial cations. These 19 bonds must come from 4^+ charges and thus the average bond valence required by the cluster is $4/19 = 0.22$ v.u.; this is the basicity of the structural unit in goedkenite. Examination of the table of Lewis acid strengths (Table 1) shows that the cations of appropriate Lewis acidity are Pb (0.20 v.u.), Sr (0.24 v.u.) and Ba (0.20 v.u.); in agreement with this, Sr is the interstitial cation in goedkenite.

(H_2O) as a bond-valence transformer

Let a cation, M , bond to an anion X [Fig. 25(a)]; the anion X receives a bond valence of v valence

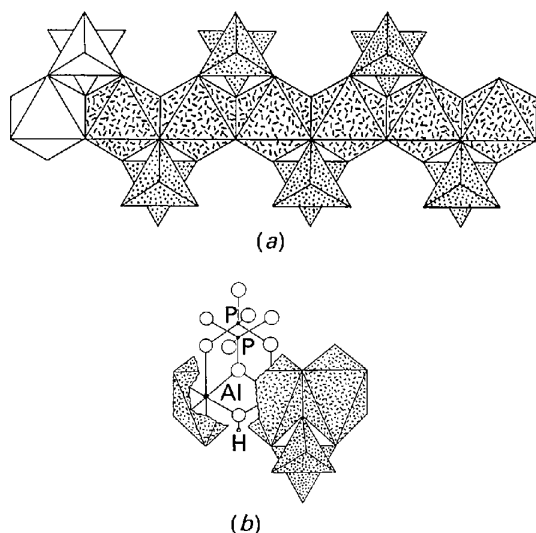


Fig. 24. The bond network in the structural unit of goedkenite.

units from the cation M . Consider a cation, M , that bonds to an (H_2O) group, which in turn bonds to an anion X [Fig. 25(b)]. In the second case, the O receives a bond-valence of v valence units from the cation M and its bond-valence requirements are satisfied by two short O—H bonds of valence $(1 - v/2)$ v.u. To satisfy the bond-valence requirements around each H atom, each H forms at least one hydrogen bond with its neighboring anions. In Fig. 25(b), one of these hydrogen bonds is to the X anion, which thus receives a bond valence of one half what it received when it was bonded directly to the M cation. Thus, the (H_2O) group acts as a *bond-valence transformer*, causing one bond (bond valence = v v.u.) to be split into two weaker bonds (bond valence = $v/2$ v.u.). It is this transformer effect that is the key to understanding the role of interstitial (H_2O) in crystals.

Interstitial (H_2O)

Interstitial (H_2O) may coordinate interstitial cations or it may occur solely as a component of a hydrogen-bonded network. Whichever is the case, the (H_2O) occupies fixed atomic positions and must play a role in the stability of the structure. The key to understanding this role is found in two distinct ideas of bond-valence theory:

- (H_2O) as a bond-valence transformer and
- application of the valence-matching principle to the interaction between the structural unit and the interstitial cations.

Ideally, the valence of the bonds from the interstitial cations to the structural unit must match the

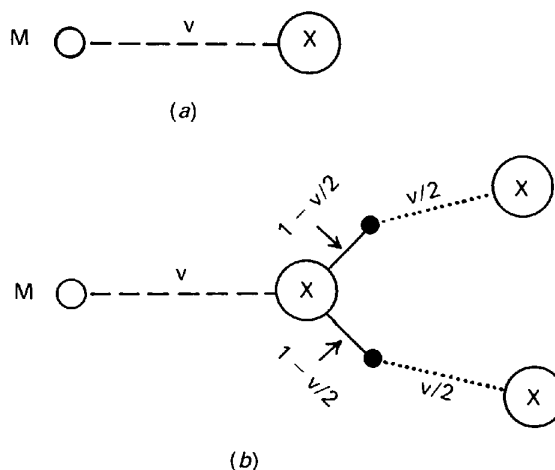


Fig. 25. The transformer effect of (H_2O) groups: (a) a cation M bonds to an oxygen X with bond valence v ; (b) a cation M bonds to an oxygen X of an (H_2O) group, and the strong bond is split into two weaker bonds (hydrogen bonds) via the bond-valence requirements of the constituent H^+ and O^{2-} ions; ● = H atom.

Lewis basicity of that structural unit; if they do not match, then there cannot be a stable interaction and that particular structural arrangement will not occur. However, if the Lewis acidity of the interstitial cation is too large, the cation may bond to an interstitial (H₂O) group, which acts as a bond-valence transformer, taking the strong bond and transforming it into two weaker bonds (Fig. 25). In this way, incorporation of interstitial (H₂O) into the structure can moderate the Lewis acidity of the interstitial cations such that the valence-matching principle is satisfied.

Consider the hydroxy-hydrated ferric-iron sulphate mineral botryogen (Süsse, 1968), Mg₂[Fe³⁺(SO₄)₄(OH)₂(H₂O)₂](H₂O)₁₀; why does this mineral have 10 interstitial (H₂O) groups per structural formula? The coordinations of the various anions in the structural unit are shown in Table 10. Using the ideal coordination numbers discussed earlier (= 3 for all the simple anions in botryogen), the structural unit needs an additional 26 bonds to achieve ideal coordination of all its simple anions. Six of these bonds will be hydrogen bonds from (OH) and (H₂O) groups within the structural unit or in adjacent structural units, leaving 20 bonds needed from interstitial cations. Thus, the Lewis basicity of the structural unit in botryogen is the charge divided by the number of required bonds: 4/20 = 0.20 v.u. The interstitial cations in botryogen are Mg, with a Lewis acidity of 0.36 v.u. The valence-matching principle is violated and a stable structure should not form. However, the interstitial Mg atoms are coordinated by {5(H₂O) + O}, and this will moderate the effective Lewis acidity of the cation via the transformer effect of (H₂O). The effective Lewis acidity of the 'complex cation' {Mg(H₂O)₅O} is the charge divided by the number of bonds:

$2/(5 \times 2 + 1) = 0.19$ v.u. The moderated Lewis acidity of the complex interstitial cation matches the Lewis basicity of the structural unit and a stable structure is formed.

Bond-valence controls on interstitial cations

Apart from the requirement of electroneutrality, the factors that govern the identity of the interstitial cations are obscure. In synthetic crystals, this point is less obvious than in minerals. When synthesizing crystals, we select the chemical systems used, thereby excluding other components from the crystal. This is not the case for minerals. Here, the chemical system is often extremely large and the crystallizing structure has access to a large variety of possible constituents. However, inspection of mineral compositions from a wide variety of chemical environments and geographical locations shows that a specific structure type can have extreme selectivity in the incorporation

Table 10. *Details of H₂O 'of hydration' in botryogen*

Botryogen: Mg₂[Fe³⁺(SO₄)₄(OH)₂(H₂O)₂](H₂O)₁₀

Bonded atoms	Number of anions	Ideal coordination no.	Bonds needed for ideal coordination
S	10	3	2 × 10
S + Fe ³⁺	6	3	1 × 6
2Fe ³⁺ + H	2	3	0
Fe ³⁺ + 2H	2	3	0

Bonds needed to structural unit = 2 × 10 + 1 × 6 = 26.

No. of hydrogen bonds to structural unit = 2 × 2 + 2 × 1 = 6.

No. of additional bonds needed = 26 - 6 = 20.

Charge on structural unit = 4⁻.

Lewis basicity of structural unit = 4/20 = 0.20 v.u.

Interstitial cation(s) is Mg.

Mg coordination = {5H₂O + O}.

Bonds from Mg to structural unit = 5 × 2 + 1 = 11.

Effective Lewis acidity of Mg = 2/{5 × 2 + 1} = 0.19 v.u.

The interstitial (H₂O) has moderated the Lewis acidity of the interstitial cation such that the valence-matching principle is satisfied.

of interstitial cations. Table 11 shows minerals of general stoichiometries [M²⁺(T⁵⁺O₄)₂(H₂O)₂] and [M²⁺(T⁵⁺O₄)₂(H₂O)]. Both contain interstitial divalent (M²⁺) cations and yet the interstitial cations seem mutually exclusive between the two groups (it should be emphasized that this is *not* a geochemical feature; both sets of cations were often available for incorporation into these structures). The analogous situation in synthetic materials is the nonisostructural nature of analogous isochemical Ca-(Sr,Ba,Pb²⁺) compounds.

So what makes the nature of the interstitial species so sensitive to the character of the structural unit? We find the answer to this problem in the application of the valence-matching principle to our binary representation of structure. The Lewis acidity of the interstitial cation must match with the basicity of the structural unit. It is not enough that the interstitial cation have the correct valence, it must also have the correct Lewis acidity. Let us examine the example outlined in the previous paragraph, that is the identity of the interstitial cations in the [M²⁺(T⁵⁺O₄)₂(H₂O)₂] and [M²⁺(T⁵⁺O₄)(H₂O)] structures, using brandtite and brackebuschite as examples.

The situation for brandtite (Hawthorne & Ferguson, 1977) is shown in Table 12; counting the bonds within the structural unit indicates that an additional 18 bonds to the structural unit are needed to attain the requisite simple anion coordination numbers. Four of these bonds are hydrogen bonds from other structural units, leaving 14 bonds to be contributed by the interstitial cations. The residual charge on the structural unit is 4⁻ (per [Mn²⁺(AsO₄)₂(H₂O)₂] unit) and hence the basicity of the structural unit is 4/14 = 0.29 v.u. Inspection of the Lewis acidity table (Table 1) shows that Ca has a Lewis acidity of 0.29 v.u., in

Table 11. Minerals with chain units of stoichiometry $[M^{2+}(T^{5+}O_4)_2(H_2O)_2]$ and $[M^{2+}(T^{5+.6+}O_4)_2(H_2O,OH)]$

	$[M^{2+}(T^{5+}O_4)_2(H_2O)_2]$		$[M^{2+}(T^{5+.6+}O_4)_2(H_2O,OH)]$
Brandtite	$Ca_2[Mn(AsO_4)_2(H_2O)_2]$	Arsenbrackebuschite	$Pb_2[Fe^{2+}(AsO_4)_2(H_2O)]$
Kröhnkite*	$Na_2[Cu(SO_4)_2(H_2O)_2]$	Arsentsumebite	$Pb_2[Cu(SO_4)(AsO_4)(OH)]$
Roselite	$Ca_2[Co(AsO_4)_2(H_2O)_2]$	Brackebuschite	$Pb_2[Mn(VO_4)_2(H_2O)]$
		Gamagarite	$Ba_2[(Fe^{3+}, Mn)(VO_4)_2(OH, H_2O)]$
Cassidyite	$Ca_2[Ni(PO_4)_2(H_2O)_2]$	Goedkenite	$Sr_2[Al(PO_4)_2(OH)]$
Collinsite	$Ca_2[Mg(PO_4)_2(H_2O)_2]$	Tsumebite	$Pb_2[Cu(PO_4)(SO_4)(OH)]$
Gaitite	$Ca_2[Zn(AsO_4)_2(H_2O)_2]$		
Roselite-beta	$Ca_2[Co(AsO_4)_2(H_2O)_2]$	Fornacite	$Pb_2[Cu(AsO_4)(CrO_4)(OH)]$
Talmselite	$Ca_2[Mg(AsO_4)_2(H_2O)_2]$	Molybdoformacite	$Pb_2[Cu(AsO_4)(MoO_4)(OH)]$
		Tornebohmite*	$\dagger(RE)_2[Al(SiO_4)_2(OH)]$
Fairfieldite	$Ca_2[Mn(PO_4)_2(H_2O)_2]$		
Messelite	$Ca_2[Fe^{2+}(PO_4)_2(H_2O)_2]$	Vauquelinite	$Pb_2[Cu(PO_4)(CrO_4)(OH)]$

* The different valence cations in the structural units of kröhnkite and tornebohmite force different valence interstitial cations for these two minerals.

† RE = rare earth atoms.

Table 12. Calculation of structural-unit basicity for brandtite and brackebuschite

Brandtite = $Ca_2[Mn^{2+}(AsO_4)_2(H_2O)_2]$ Structural unit = $[Mn^{6l}(As^{6l}O_4)_2(H^{2l}O)_2]$

Number of bonds in structural unit = $1 \times [6] + 2 \times [4] + 2 \times [2] = 18$

Number of bonds needed for four-coordination of all simple anions (except

H_2O for which three-coordination is assigned = $8 \times [4] + 2 \times [3] = 38$

Number of additional bonds to structural unit to achieve this coordination = 20

Number of hydrogen bonds to structural unit = $2 \times 2 = 4$

Therefore, the number of bonds required from interstitial cations = $20 - 4 = 16$

Charge on the structural unit $[Mn^{2+}(AsO_4)_2(H_2O)_2]$ in brandtite = 4

Lewis basicity of structural unit = charge/bonds = $4/16 = 0.25$ v.u.

This basicity matches most closely with the Lewis acidity of Ca at 0.27 v.u.

Thus, the formula of brandtite is $Ca_2[Mn(AsO_4)_2(H_2O)_2]$

Brackebuschite = $Pb_2[Mn^{2+}(VO_4)_2(H_2O)]$ Structural unit = $[Mn^{6l}(V^{6l}O_4)_2(H^{2l}O)]$

Number of bonds in structural unit = $1 \times [6] + 2 \times [4] + 2 \times [1] = 16$

Number of bonds needed for four-coordination of all simple anions

(including H_2O which is four-coordinated in this structural unit) = $9 \times [4] = 36$

Number of additional bonds to structural unit to achieve this coordination = 20

Number of hydrogen bonds to structural unit = 2

Number of bonds required from interstitial cations = 18

Charge on the structural unit $[Mn^{2+}(VO_4)_2(H_2O)]$ in brackebuschite = 4

Lewis basicity of structural unit = charge/bonds = $4/18 = 0.22$ v.u.

This basicity matches most closely with the Lewis acidity of Pb at 0.20 v.u.

Thus, the formula of brackebuschite is $Pb_2[Mn(VO_4)_2(H_2O)]$

exact agreement with the Lewis basicity of the structural unit. Hence, the valence-matching principle is satisfied, and $Ca_2[Mn^{2+}(AsO_4)_2(H_2O)_2]$ is a stable structure.

Brackebuschite (Donaldson & Barnes, 1955) is also shown in Table 12; an additional 20 bonds are needed to satisfy the requisite simple anion coordination requirements. Two of these bonds are hydrogen bonds from adjacent structural units, leaving 18 bonds to be satisfied by interstitial cations. The residual charge on the structural unit is 4^- and hence the basicity of the structural unit is $4/18 = 0.22$ v.u. This value matches up quite well with the Lewis basicity of Pb^{2+} (0.20 v.u., see Table 1), the valence-matching principle is satisfied and $Pb^{2+}[Mn^{2+}(V^{5+}O_4)_2(H_2O)]$ is a stable structure.

Some very interesting questions now become apparent concerning the nature of crystallization. Does the form of the structural unit dictate the identity of the interstitial cations, or does the availability of a particular interstitial cation dictate the form of the structural unit? Does the pH of the environment affect the form of the structural unit or the amount of interstitial (H_2O) incorporated into the structure? Are there synergetic interactions between these factors? Using bond-valence theory in conjunction with the topological characteristics of the structural unit, we can begin to investigate some of these questions.

Summary

Bond topology has a major effect on the energetics of a structure, suggesting that major trends in structure stability, properties and behavior should be systematically related to the coordination geometry and polyhedral linkage of a structure. Combination of these ideas with bond-valence theory (a very simple form of molecular-orbital theory) allows simple binary representation of even the most complex structure: a (usually anionic) structural unit that interacts with (usually cationic or neutral) interstitial species to form the complete structure. This interaction can be quantitatively examined in terms of the Lewis basicities and acidities of the binary components; such features as interstitial cation chemistry and 'water' of hydration can be explained and quantitative predictions can be made.

The principal idea behind this work is to develop an approach that is reasonably transparent to chemical and physical intuition, and that can be applied to large numbers of very complex structures. There is a need for a simple approach that addresses the more global aspects of complex oxysalt structures. These ideas tend to be intuitive and semiquantitative, but are capable of organizing a large amount of informa-

tion into a coherent framework, and also provide a basis for thinking about many questions that were intractable to previous approaches.

This work was supported by a Killam Fellowship and by the Natural Sciences and Engineering Council of Canada in the form of an Operating Grant to the author.

References

- AKAO, M. & IWAI, S. (1977). *Acta Cryst.* B33, 3951–3953.
- AKPORIAYE, D. E. & PRICE, G. D. (1989). *Zeolites* 9, 23–35.
- ALBRIGHT, T. A., BURDETT, J. K. & WHANGBO, M. H. (1985). *Orbital Interactions in Chemistry*. New York: Wiley-Interscience.
- ALLMANN, R. (1975). *Monatsh. Chem.* 106, 779–793.
- BAUR, W. H. (1970). *Trans. Am. Cryst. Assoc.* 6, 129–155.
- BAUR, W. H. (1971). *Am. Mineral.* 69, 601–621.
- BAUR, W. H. (1981). *Structure and Bonding in Crystals*, Vol. 2, edited by M. O'KEEFFE & A. NAVROTSKY, pp. 31–51. New York: Academic Press.
- BAUR, W. H. (1987). *Cryst. Rev.* 1, 59–83.
- BLOCH, A. N. & SCHATTEMAN, G. C. (1981). *Structure and Bonding in Crystals*, Vol. 1, edited by M. O'KEEFFE & A. NAVROTSKY, pp. 49–72. New York: Academic Press.
- BORNE, J. (1970). *Bull. Soc. Mineral. Cryst.* 93, 185–189.
- BORN, M. & LANDÉ, A. (1918). *Sitzungsber. Preuss. Akad. Wiss. Berlin*, 45, 1048–1068.
- BRAGG, W. L. (1913). *Proc. R. Soc. Sect. A*, 89, 248–263.
- BRAGG, W. L. (1921). *Sci. Prog.* 16, 45–55.
- BRAGG, W. L. (1930). *Z. Kristallogr.* 74, 237–305.
- BRAGG, W. L. (1955). *The Crystalline State. A General Survey*. London: G. Bell & Sons Ltd.
- BROWN, I. D. (1976). *Acta Cryst.* A32, 224–231.
- BROWN, I. D. (1981). *Structure and Bonding in Crystals*, Vol. 2, edited by M. O'KEEFFE & A. NAVROTSKY, pp. 1–30. New York: Academic Press.
- BROWN, I. D. (1988). *Acta Cryst.* B44, 545–553.
- BROWN, I. D. (1992). *Acta Cryst.* B48, 553–572.
- BROWN, I. D. & SHANNON, R. D. (1973). *Acta Cryst.* A29, 266–282.
- BRUNNER, G. O. & MEIER, W. M. (1989). *Nature*, 337, 146–147.
- BUCAT, R. B., PATRICK, J. M., WHITE, A. H. & WILLIS, A. C. (1977). *Aust. J. Chem.* 30, 1379–1382.
- BURDETT, J. K. (1980). *Molecular Shapes*. New York: Wiley.
- BURDETT, J. K. (1986). *Mol. Struct. Energ.* 1, 209–275.
- BURDETT, J. K. (1987). *Struct. Bonding*, 65, 30–90.
- BURDETT, J. K. & HAWTHORNE, F. C. (1993). *Am. Mineral.* 78, 884–892.
- BURDETT, J. K., LEE, S. & SHA, W. C. (1984). *Croat. Chem. Acta*, 57, 1193–1216.
- BURDETT, J. K. & McLARNAN, T. J. (1984). *Am. Mineral.* 69, 601–621.
- BURDETT, J. K., PRICE, G. D. & PRICE, S. L. (1981). *Phys. Rev. B*, 24, 2903–2912.
- BURNHAM, C. W. (1990). *Am. Mineral.* 75, 443–463.
- CATLOW, C. R. A. & PRICE, G. D. (1990). *Nature*, 347, 243–248.
- CERNY, P. & HAWTHORNE, F. C. (1976). *Can. Mineral.* 14, 491–497.
- CHRIST, C. L. (1960). *Am. Mineral.* 45, 334–340.
- CHRIST, C. L. & CLARK, J. R. (1977). *Phys. Chem. Mineral.* 2, 59–87.
- COHEN, M. L. (1981). *Structure and Bonding in Crystals*, Vol. 1, edited by M. O'KEEFFE & A. NAVROTSKY, pp. 25–48. New York: Academic Press.
- CROMER, D. T., KAY, M. I. & LARSEN, A. C. (1967). *Acta Cryst.* 22, 182–187.
- DENT GLASSER, L. S. (1979). *Z. Kristallogr.* 149, 291–305.
- DONALDSON, D. M. & BARNES, W. H. (1955). *Am. Mineral.* 40, 597–613.
- DOVE, M. T., WINKLER, B., LESLIE, M., HARRIS, M. J. & SALJE, E. K. H. (1992). *Am. Mineral.* 77, 244–250.
- DOVESI, R., PISANI, C., ROETTI, C. & SILVI, B. (1987). *J. Chem. Phys.* 86, 6967–6971.
- EBY, R. K. & HAWTHORNE, F. C. (1993). *Acta Cryst.* B49, 28–56.
- EMSLEY, J., JONES, D. H. & LUCAS, J. (1981). *Rev. Inorg. Chem.* 3, 105–140.
- FANFANI, L., NUNZI, A. & ZANAZZI, P. F. (1970). *Am. Mineral.* 55, 78–89.
- FANFANI, L., NUNZI, A. & ZANAZZI, P. F. (1971). *Am. Mineral.* 56, 751–757.
- FERRARIS, G. & FRANCHINI-ANGELA, M. (1972). *Acta Cryst.* B28, 3572–3583.
- FINNIS, M. W., PAXTON, A. T., PETTIFOR, D. G., SUTTON, A. P. & OHTA, Y. (1988). *Phil. Mag.* 58, 143–163.
- GIACOVAZZO, G., SCORDARI, F., TODISCO, A. & MENCHETTI, S. (1976). *Tschermaks Mineral. Petrogr. Mitt.* 23, 155–165.
- GIBBS, G. V. (1982). *Am. Mineral.* 67, 421–450.
- GIBBS, G. V., BRECK, D. W. & MEAGHER, E. P. (1968). *Lithos*, 1, 275–285.
- GIBBS, G. V., HAMIL, M. M., LOUISNATHAN, S. J., BARTELL, L. S. & YOW, H. (1972). *Am. Mineral.* 57, 1578–1613.
- GIUSEPPETTI, E. & TADINI, C. (1984). *Neues Jahrb. Mineral Monatsh.* pp. 263–271.
- GOLDSCHMIDT, V. M. (1928). *Z. Phys. Chem.* 133, 397–417.
- GOLDSCHMIDT, V. M. (1954). *Geochemistry*. Oxford: Clarendon Press.
- GORDON, R. G. & KIM, Y. S. (1972). *J. Chem. Phys.* 56, 3122–3133.
- HAWTHORNE, F. C. (1979). *Can. Mineral.* 17, 93–102.
- HAWTHORNE, F. C. (1983). *Acta Cryst.* A39, 724–736.
- HAWTHORNE, F. C. (1984a). *Can. Mineral.* 22, 245–251.
- HAWTHORNE, F. C. (1984b). *Can. Mineral.* 22, 475–480.
- HAWTHORNE, F. C. (1985a). *Am. Mineral.* 70, 455–473.
- HAWTHORNE, F. C. (1985b). *Tschermaks Mineral. Petrogr. Mitt.* 34, 15–34.
- HAWTHORNE, F. C. (1985c). *Can. Mineral.* 23, 669–674.
- HAWTHORNE, F. C. (1986). *Can. Mineral.* 24, 625–642.
- HAWTHORNE, F. C. (1990). *Z. Kristallogr.* 192, 1–52.
- HAWTHORNE, F. C. (1992). *Z. Kristallogr.* 201, 183–206.
- HAWTHORNE, F. C. & CERNY, P. (1977). *Can. Mineral.* 15, 414–421.
- HAWTHORNE, F. C. & FAGGIANI, R. (1979). *Acta Cryst.* B35, 717–720.
- HAWTHORNE, F. C. & FERGUSON, R. B. (1975a). *Can. Mineral.* 13, 181–187.
- HAWTHORNE, F. C. & FERGUSON, R. B. (1975b). *Can. Mineral.* 13, 289–291.
- HAWTHORNE, F. C. & FERGUSON, R. B. (1977). *Can. Mineral.* 15, 36–42.
- HAWTHORNE, F. C., GROAT, L. A., RAUDSEPP, M. & ERCIT, T. S. (1987). *Neues Jahrb. Mineral. Abh.* 157, 121–132.
- HOFFMANN, R. (1988). *Solids and Surfaces: a Chemist's View of Bonding in Extended Structures*. New York: VCH Publishers.
- HOPPE, R. (1981). *Angew. Chem.* 19, 110–125.
- KAMPE, A. R. (1977). *Am. Mineral.* 62, 256–262.
- KAMPE, A. R. & MOORE, P. B. (1976). *Am. Mineral.* 61, 1241–1248.
- LEWIS, G. N. (1916). *J. Am. Chem. Soc.* 38, 762–785.
- LEWIS, G. N. (1923). *Valence and the Structure of Atoms and Molecules*. New York: American Chemical Society Monograph Series.
- LIEBAU, F. (1985). *Structure Chemistry of Silicates*. Berlin: Springer Verlag.

- LIMA DE FARIA, J. (1983). *Garcia de Orta, série Geol.* **6**, 1–14.
- LIMA DE FARIA, J. & FIGUEIREDO, M. O. (1976). *J. Solid State Chem.* **16**, 7–20.
- LIMA DE FARIA, J., HELLNER, E., LIEBAU, F., MAKOVICKY, E. & PARTHÉ, E. (1990). *Acta Cryst.* **A46**, 1–11.
- MADDOX, J. (1988). *Nature*, **335**, 201.
- MADELUNG, E. (1918). *Phys. Z.* **19**, 524–532.
- MEREITER, K. (1974). *Tschermaks Mineral. Petrogr. Mitt.* **21**, 216–232.
- MOORE, P. B. (1970a). *Neues Jahrb. Mineral. Monatsh.* **1970**, 163–173.
- MOORE, P. B. (1970b). *Am. Mineral.* **55**, 135–169.
- MOORE, P. B. (1973). *Mineral. Rec.* **4**, 103–130.
- MOORE, P. B. (1974). *Neues Jahrb. Mineral. Abh.* **120**, 205–227.
- MOORE, P. B. (1975). *Neues Jahrb. Mineral. Abh.* **123**, 148–159.
- MOORE, P. B. (1981). *Bull. Mineral.* **104**, 536–547.
- MOORE, P. B. (1982). *Mineral. Assoc. Can. Short Course* **8**, 267–291.
- MOORE, P. B. (1984). Crystallochemical aspects of the phosphate minerals. In *Phosphate Minerals*, edited by J. O. NIAGRU & P. B. MOORE, pp. 155–170. Berlin: Springer-Verlag.
- MOORE, P. B. & ARAKI, T. (1972). *Am. Mineral.* **57**, 1355–1374.
- MOORE, P. B., ARAKI, T., KAMPF, A. R. & STEELE, I. M. (1976). *Am. Mineral.* **61**, 5–11.
- MOORE, P. B., IRVING, A. J. & KAMPF, A. R. (1975). *Am. Mineral.* **60**, 957–964.
- MOORE, P. B., KAMPF, A. R. & IRVING, A. J. (1974). *Am. Mineral.* **59**, 900–905.
- MULLER, O. & ROY, R. (1974). *The Major Ternary Structural Families*. New York: Springer-Verlag.
- O'KEEFFE, M. (1989). *Struct. Bonding*, **71**, 161–191.
- O'KEEFFE, M. (1990). *Acta Cryst.* **A46**, 138–142.
- O'KEEFFE, M. & BRESE, N. E. (1991). *J. Am. Chem. Soc.* **113**, 3226–3229.
- O'KEEFFE, M. & HYDE, B. G. (1980). *Phil. Trans. R. Soc. London*, **295**, 553–623.
- O'KEEFFE, M. & HYDE, B. G. (1984). *Nature*, **309**, 411–414.
- PABST, A. (1950). *Am. Mineral.* **35**, 149–165.
- PATEL, A., PRICE, G. D. & MENDELSSOHN, M. J. (1991). *Phys. Chem. Mineral.* **17**, 690–699.
- PAULING, L. (1929). *J. Am. Chem. Soc.* **51**, 1010–1026.
- PAULING, L. (1960). *The Nature of the Chemical Bond*, 3rd ed. Ithaca, New York: Cornell University Press.
- PHILLIPS, J. C. (1970). *Rev. Mod. Phys.* **42**, 317–356.
- PHILLIPS, J. C. (1973). *Bonds and Bands in Semiconductors*. New York: Academic Press.
- PISANI, C. (1987). *Int. Rev. Phys. Chem.* **6**, 367–384.
- RIPMEESTER, J. A., RATCLIFFE, C. I., DUTRIZAC, J. E. & JAMBOR, J. L. (1986). *Can. Mineral.* **24**, 435–447.
- SABELLI, C. (1985a). *Z. Kristallogr.* **173**, 33–39.
- SABELLI, C. (1985b). *Bull. Minéral.* **108**, 133–138.
- SCORDARI, F. (1980). *Mineral. Mag.* **43**, 669–673.
- SCORDARI, F. (1981). *Tschermaks Mineral. Petrogr. Mitt.* **28**, 207–222.
- SHANNON, R. D. (1975). Systematic studies of interatomic distances in oxides. In *The Physics and Chemistry of Minerals and Rocks*, edited by R. G. J. STRENS, pp. 403–431. London: John Wiley & Sons.
- SHANNON, R. D. (1976). *Acta Cryst.* **A32**, 751–767.
- SHANNON, R. D. & PREWITT, C. T. (1970). *J. Solid State Chem.* **2**, 199–202.
- SHANNON, R. D., SUBRAMANIAN, M. A., MARIANO, A. N., GIER, T. E. & ROSSMAN, G. R. (1992). *Am. Mineral.* **77**, 101–106.
- SIMONS, G. & BLOCH, A. N. (1973). *Phys. Rev. B*, **7**, 2754–2761.
- SMITH, J. V. (1977). *Am. Mineral.* **62**, 703–709.
- SMITH, J. V. (1988). *Chem. Rev.* **188**, 149–182.
- SRIVASTAVA, G. P. & WEAIRE, D. (1987). *Adv. Phys.* **36**, 463–517.
- STEPHENS, J. S. & CRUICKSHANK, D. W. J. (1970). *Acta Cryst.* **B26**, 222–226.
- SÜSSE, P. (1968). *Acta Cryst.* **B24**, 760–767.
- SUTOR, D. J. (1967). *Acta Cryst.* **23**, 418–422.
- TILLMANN, E. & GEBERT, W. (1973). *Acta Cryst.* **B29**, 2789–2794.
- TOSSELL, J. A. & GIBBS, G. V. (1977). *Phys. Chem. Mineral.* **2**, 21–57.
- TOSSELL, J. A. & VAUGHAN, D. J. (1992). *Theoretical Geochemistry: Applications of Quantum Mechanics in the Earth and Mineral Sciences*. Oxford: Oxford University Press.
- TRINAJSTIC, N. (1983). *Chemical Graph Theory*, Vol. I. Boca Raton: CRC Press.
- WELLS, A. F. (1956). *The Third Dimension in Chemistry*. Oxford: Clarendon Press.
- WELLS, A. F. (1970). *Models in Structural Inorganic Chemistry*. Oxford: Oxford University Press.
- WELLS, A. F. (1977). *Three-Dimensional Nets and Polyhedra*. New York: John Wiley & Sons.
- WELLS, A. F. (1984). *Structural Inorganic Chemistry*, 5th ed. Oxford: Oxford University Press.
- WOOD, I. G. & PRICE, G. D. (1992). *Zeolites*, **12**, 320–327.
- YA-HSIEN, K., SIMONOV, V. I. & BELOV, N. V. (1963). *Dokl. Akad. Nauk SSSR*, **149**, 123–126.
- ZAHROBSKY, R. F. & BAUR, W. H. (1968). *Acta Cryst.* **B24**, 508–513.
- ZIMAN, J. (1965). *Principles of the Theory of Solids*. Cambridge: Cambridge University Press.
- ZOLTAI, T. (1960). *Am. Mineral.* **45**, 960–973.
- ZUNGER, A. (1981). *Structure and Bonding in Crystals*, Vol. 1, edited by M. O'KEEFFE & A. NAVROTSKY, pp. 73–135. New York: Academic Press.
- ZUNGER, A. & COHEN, M. L. (1978). *Phys. Rev. B*, **18**, 5449–5472.
- ZUNGER, A. & COHEN, M. L. (1979). *Phys. Rev. B*, **20**, 4082–4108.